

Environmental Applications of Semiconductor Photocatalysis

Michael R. Hoffmann,* Scot T. Martin, Wonyong Choi, and Detlef W. Bahnemann†

W. M. Keck Laboratories, California Institute of Technology, Pasadena, California 91125

Received October 21, 1994 (Revised Manuscript Received November 30, 1994)

Contents

I. Introduction	69
A. General Background	69
B. Semiconductor Photocatalysis	70
II. Mechanisms of Semiconductor Photocatalysis	71
A. Basic Features and Characteristic Times	71
B. Formation of Reactive Oxygen Species	73
III. Chemical Kinetics of Semiconductor Photocatalysis	74
A. Heterogeneous Photochemical Kinetics	74
1. Reaction Stoichiometry	74
2. Reaction Rates, Surface Interactions, and Quantum Efficiencies	75
B. Surface Chemistry of Metal Oxide Semiconductors	75
C. Langmuir–Hinshelwood Kinetics	77
D. Heterogeneous Quantum Efficiencies	78
E. Sorption of Electron Donors and Acceptors	79
IV. Bulk-Phase Semiconductors	79
A. Metal Oxide Semiconductors and TiO ₂	79
B. Metal Ion Dopants and Bulk-Phase Photoreactivity	80
V. Quantum-Sized Semiconductors	80
A. Basic Characteristics and Behavior	80
B. Doped Quantum-Sized TiO ₂	81
VI. Photochemical Reactors	82
A. Water Treatment Systems	82
B. Gas-Phase Treatment Systems	83
VII. Important Reaction Variables	83
VIII. Photochemical Transformation of Specific Compounds	85
A. Inorganic Compounds	85
B. Organic Compounds	85
IX. Mechanistic Aspects of Selected Reactions	87
A. Chloroform	87
B. Pentachlorophenol	87
C. Glyoxylic Acid	88
D. Acetic Acid	88
E. Carbon Tetrachloride	89
F. 4-Chlorophenol	90
X. Conclusions	91
XI. Acknowledgments	91
XII. References	91

I. Introduction

A. General Background

The civilian, commercial, and defense sectors of most advanced industrialized nations are faced with

a tremendous set of environmental problems related to the remediation of hazardous wastes, contaminated groundwaters, and the control of toxic air contaminants. For example, the slow pace of hazardous waste remediation at military installations around the world is causing a serious delay in conversion of many of these facilities to civilian uses. Over the last 10 years problems related to hazardous waste remediation¹ have emerged as a high national and international priority.

Problems with hazardous wastes at military installations are related in part to the disposal of chemical wastes in lagoons, underground storage tanks, and dump sites. As a consequence of these disposal practices, the surrounding soil and underlying groundwater aquifers have become contaminated with a variety of hazardous (i.e., toxic) chemicals. Typical wastes of concern include heavy metals, aviation fuel, military-vehicle fuel, solvents and degreasing agents, and chemical byproducts from weapons manufacturing. The projected costs for cleanup at more than 1800 military installations in the United States have been put at \$30 billion; the time required for cleanup has been estimated to be more than 10 years.

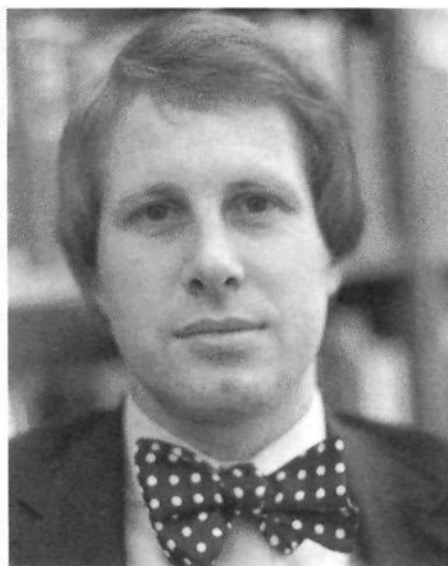
In the civilian sector, the elimination of toxic and hazardous chemical substances such as the halogenated hydrocarbons from waste effluents and previously contaminated sites has become a major concern. More than 540 million metric tons of hazardous solid and liquid waste are generated annually by more than 14000 installations in the United States. A significant fraction of these wastes are disposed on the land each year. Some of these wastes eventually contaminate groundwater and surface water.

Groundwater contamination is likely to be the primary source of human contact with toxic chemicals emanating from more than 70% of the hazardous waste sites in the United States. General classes of compounds of concern include: solvents, volatile organics, chlorinated volatile organics, dioxins, dibenzofurans, pesticides, PCB's, chlorophenols, asbestos, heavy metals, and arsenic compounds. Some specific compounds of interest are 4-chlorophenol, pentachlorophenol, trichloroethylene (TCE), perchloroethylene (PCE), CCl₄, HCCl₃, CH₂Cl₂, ethylene dibromide, vinyl chloride, ethylene dichloride, methyl chloroform, *p*-chlorobenzene, and hexachlorocyclopentadiene. The occurrence of TCE, PCE, CFC-113 (i.e., Freon-113) and other grease-cutting agents in soils and groundwaters is widespread.

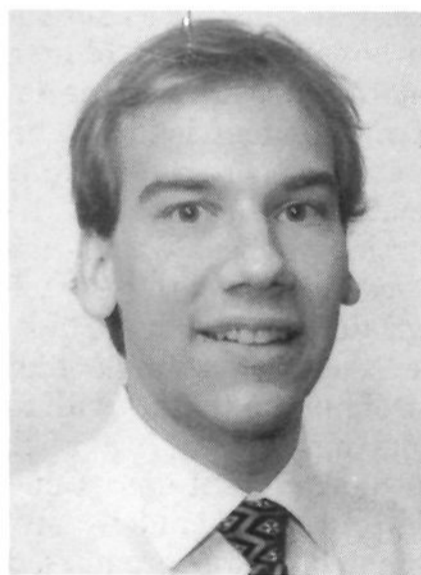
In order to address this significant problem, extensive research is underway to develop advanced analytical, biochemical, and physicochemical methods for the characterization and elimination of hazardous chemical compounds from air, soil, and water. Advanced physicochemical processes such as semicon-

* Author to whom correspondence should be addressed.

† Institute for Solar Energy Research, Hannover, D-30165, Germany.



Dr. Hoffmann was born in Fond du Lac, WI, in 1946. He received a B.S. degree in chemistry in 1968 from Northwestern University, a Ph.D. degree in chemical kinetics from Brown University in 1973, and postdoctoral training in Environmental Engineering at the California Institute of Technology from 1973 to 1975. Dr. Hoffmann has been a Professor of Environmental Engineering and Environmental Chemistry since 1975. From 1975 to 1980, he was member of the faculty at the University of Minnesota and since 1980 a member of the faculty at Caltech (Engineering & Applied Science). Dr. Hoffmann has published more than 140 peer-reviewed professional papers and is the holder of five patents in the subject areas of applied chemical kinetics, environmental chemistry, catalytic oxidation, heterogeneous photochemistry, and applied microbial catalysis. Dr. Hoffmann has served as the Chairman of the Gordon Research Conference, Environmental Sciences; Water, as the Associate Editor of the *Journal of Geophysical Research*. He is currently on the Members Board of the National Center for Atmospheric Research and the Editorial Board of *Environmental Science and Technology*. Dr. Hoffmann has spent the summers of 1992–1995 in Germany as an Alexander von Humboldt Prize recipient at the Max Planck Institute for Chemistry in Mainz, the Institute for Solar Energy Research in Hannover, and the Institute for Inorganic Chemistry at the University of Erlangen/Nürnberg. (Photo by Bob Paz, Caltech.)



Scot T. Martin was born in Indianapolis, IN, and attended Georgetown University, Washington, DC (B.S. Chemistry, 1991). He spent one year studying chemistry at Oxford University. He is currently completing his Ph.D. with Professor Michael R. Hoffmann at the California Institute of Technology. During this time he has been supported by a National Defense Science and Engineering Graduate Fellowship. He is the recipient of the ACS Graduate Student Paper Award in the Division of Environmental Chemistry. His research interests include environmental heterogeneous chemistry, photochemistry, and semiconductor electrochemistry.

ductor photocatalysis are intended to be both supplementary and complementary to some of the more conventional approaches to the destruction or transformation of hazardous chemical wastes such as high-temperature incineration, amended activated sludge digestion, anaerobic digestion, and conventional physicochemical treatment.^{1–5}



Wonyong Choi was born in Kimhae, Korea, in 1965. He received a B.S. in Engineering from the Department of Chemical Technology at Seoul National University (Seoul, Korea) in 1988 and an M.S. in Physical Chemistry from Pohang Institute of Science and Technology (Pohang, Korea) in 1990. Since 1991 he has been a graduate student at Chemistry and Environmental Engineering Science in California Institute of Technology. Under the direction of Professor Michael R. Hoffmann, he is currently studying the photoelectrochemical reactions on semiconductor colloid surfaces.



Detlef W. Bahnemann studied Chemistry at the Technical University Berlin (Germany) from 1972 to 1977, and Biochemistry at the Brunel University, Uxbridge (Great Britain) from 1976 to 1977. He received his Diploma in Chemistry from the Technical University Berlin in 1977, and his Ph.D. in Chemistry in 1981 also from the Technical University Berlin. From 1981 to 1988 he worked as a senior scientist in the group of Professor A. Henglein at the Hahn-Meitner-Institute Berlin focusing his research activities on particulate photoelectrochemistry, photocatalytic transformations of organic compounds as well as the synthesis and characterization of ultra-small metal and semiconductor particles. Between 1985 and 1987, Dr. Bahnemann worked as a visiting associate at the California Institute of Technology, Pasadena, CA, with Professor M. R. Hoffmann in the Department of Environmental Engineering. During that time he started to study free radical processes in the environment and continued his research on photocatalytic processes. Since 1988, Detlef Bahnemann has been working as the Head of the Department of Photoelectrochemistry and Material Research at the Institute for Solar Energy Research in Hannover (Germany) where he is also in charge of the Photocatalysis research group. He is Lecturer for Physical Chemistry at the University of Oldenburg and supervisor of Ph.D. and Diploma theses at the universities of Hannover, Clausthal-Zellerfeld, and Oldenburg. Current research interests include heterogeneous photocatalysis, nanocrystalline materials, solar and environmental chemistry.

B. Semiconductor Photocatalysis

Over the last 10 years the scientific and engineering interest in the application of semiconductor photocatalysis has grown exponentially. In the areas of water, air, and wastewater treatment alone, the rate of publication exceeds 200 papers per year

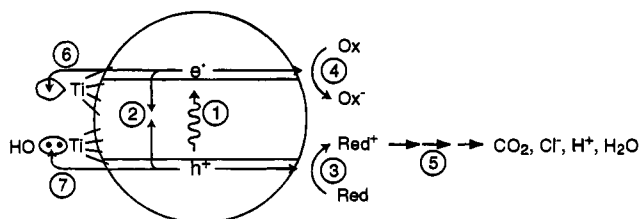


Figure 1. Primary steps in the photoelectrochemical mechanism: (1) formation of charge carriers by a photon; (2) charge carrier recombination to liberate heat; (3) initiation of an oxidative pathway by a valence-band hole; (4) initiation of a reductive pathway by a conduction-band electron; (5) further thermal (e.g., hydrolysis or reaction with active oxygen species) and photocatalytic reactions to yield mineralization products; (6) trapping of a conduction-band electron in a dangling surficial bond to yield Ti(III); (7) trapping of a valence-band hole at a surficial titanol group.

averaged over the last 10 years.⁶ In this paper, we attempt to give an overview of some of the underlying principles governing semiconductor photocatalysis and to review the current literature in terms of its potential applications as an environmental control technology.⁶

Given the tremendous level of interest in semiconductor photochemistry and photophysics over the last 15 years, a number of review articles have appeared. For additional background information and reviews of the relevant literature, we refer the reader to recent reviews provided by Ollis and Al-Akabi,⁶ Blake,⁷ Mills et al.,⁸ Kamat,⁹ Fox and Dulay,¹⁰ Bahnemann,¹¹ Pichat,¹² Aithal et al.,¹³ Lewis¹⁴ and Bahnemann et al.¹⁵ Earlier overviews are available in the works of Fox,¹⁶ Ollis et al.,¹⁷ Pelizzetti and Serpone,¹⁸ Grätzel,¹⁹ Matthews,²⁰ Schiavello,^{21,22} Serpone et al.,²³ Serpone and Pelizzetti,²⁴ Anpo,²⁵ Bahnemann et al.,²⁶ and Henglein.²⁷

Semiconductor photocatalysis with a primary focus on TiO₂ as a durable photocatalyst has been applied to a variety of problems of environmental interest in addition to water and air purification. It has been shown to be useful for the destruction of microorganisms such as bacteria²⁸ and viruses,²⁹ for the inactivation of cancer cells,^{30,31} for odor control,³² for the photosplitting of water to produce hydrogen gas,^{33–38} for the fixation of nitrogen,^{39–42} and for the clean up of oil spills.^{43–45}

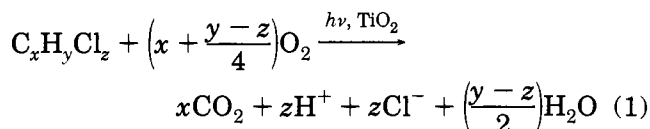
Semiconductors (e.g., TiO₂, ZnO, Fe₂O₃, CdS, and ZnS) can act as sensitizers for light-reduced redox processes due to their electronic structure, which is characterized by a filled valence band and an empty conduction band.⁴⁶ When a photon with an energy of $h\nu$ matches or exceeds the bandgap energy, E_g , of the semiconductor, an electron, e_{cb}^- , is promoted from the valence band, VB, into the conduction band, CB, leaving a hole, h_{vb}^+ behind (see Figure 1). Excited-state conduction-band electrons and valence-band holes can recombine and dissipate the input energy as heat, get trapped in metastable surface states, or react with electron donors and electron acceptors adsorbed on the semiconductor surface or within the surrounding electrical double layer of the charged particles.

In the absence of suitable electron and hole scavengers, the stored energy is dissipated within a few

nanoseconds by recombination.⁴⁷ If a suitable scavenger or surface defect state is available to trap the electron or hole, recombination is prevented and subsequent redox reactions may occur. The valence-band holes are powerful oxidants (+1.0 to +3.5 V vs NHE depending on the semiconductor and pH), while the conduction-band electrons are good reductants (+0.5 to -1.5 V vs NHE).¹⁹ Most organic photodegradation reactions utilize the oxidizing power of the holes either directly or indirectly; however, to prevent a buildup of charge one must also provide a reducible species to react with the electrons. In contrast, on bulk semiconductor electrodes only one species, either the hole or electron, is available for reaction due to band bending.⁴⁸ However, in very small semiconductor particle suspensions both species are present on the surface. Therefore, careful consideration of both the oxidative and the reductive paths is required.

The application of illuminated semiconductors for the remediation of contaminants has been used successfully for a wide variety of compounds^{49–56} such as alkanes, aliphatic alcohols, aliphatic carboxylic acids, alkenes, phenols, aromatic carboxylic acids, dyes, PCB's, simple aromatics, halogenated alkanes and alkenes, surfactants, and pesticides as well as for the reductive deposition of heavy metals (e.g., Pt⁴⁺, Au³⁺, Rh³⁺, Cr(VI)) from aqueous solution to surfaces.^{17,57–59} In many cases, complete mineralization of organic compounds has been reported.

A general stoichiometry for the heterogeneously photocatalyzed oxidation of a generic chlorinated hydrocarbon to complete mineralization can be written as follows:



II. Mechanisms of Semiconductor Photocatalysis

A. Basic Features and Characteristic Times

On the basis of laser flash photolysis measurements^{60,61} we have proposed the following general mechanism for heterogeneous photocatalysis on TiO₂. Characteristic times for the various steps in the mechanism are given to the right of each step.

Primary Process	Characteristic Times
charge-carrier generation $TiO_2 + h\nu \rightarrow h_{vb}^+ + e_{cb}^-$	(fs) (2)
charge-carrier trapping $h_{vb}^+ + >Ti^{IV}OH \rightarrow \{>Ti^{IV}OH^+\}^+$ $e_{cb}^- + >Ti^{IV}OH \leftrightarrow \{>Ti^{III}OH\}$	fast (10 ns) (3) shallow trap (100 ps) (4a) (dynamic equilibrium)
$e_{cb}^- + >Ti^{IV} \rightarrow >Ti^{III}$	deep trap (10 ns) (4b) (irreversible)
charge-carrier recombination $e_{cb}^- + \{>Ti^{IV}OH^+\}^+ \rightarrow >Ti^{IV}OH$ $h_{vb}^+ + \{>Ti^{III}OH\} \rightarrow >Ti^{IV}OH$	slow (100 ns) (5) fast (10 ns) (6)
interfacial charge transfer $\{>Ti^{IV}OH^+\}^+ + Red \rightarrow >Ti^{IV}OH + Red^+$	slow (100 ns) (7)
$e_{tr}^- + O_x \rightarrow >Ti^{IV}OH + O_x^-$	very slow (ms) (8)

where $>TiOH$ represents the primary hydrated surface functionality of TiO₂,⁶² e_{cb}^- is a conduction-band

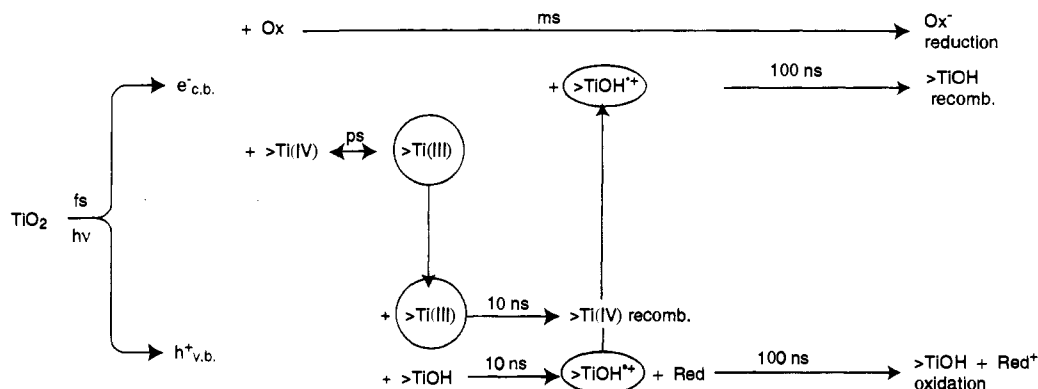


Figure 2. Kinetics of the primary steps in photoelectrochemical mechanism. Recombination is mediated primarily by >Ti(III) in the first 10 ns. Valence-band holes are sequestered as long-lived >TiOH^{•+} after 10 ns. >TiOH is reformed by recombination with conduction-band electrons or oxidation of the substrate on the time scale of 100 ns. The arrow lengths are representative of the respective time scales.

electron, e_{tr}^- is a trapped conduction-band electron, h_{vb}^+ is a valence-band hole, Red is an electron donor (i.e., reductant), Ox is an electron acceptor (i.e., oxidant), $\{>Ti^{IV}OH\}^+$ is the surface-trapped VB hole (i.e., surface-bound hydroxyl radical), and $\{>Ti^{III}OH\}$ is the surface-trapped CB electron. The dynamic equilibrium of eq 4a represents a reversible trapping of a conduction-band electron in a shallow trap below the conduction-band edge such that there is a finite probability that e_{tr}^- can be transferred back into the conduction band at room temperature. This step is plausible if we consider that kT at 25 °C is equivalent to 26 meV. Trapped electrons have been estimated to lie in the range of 25 to 50 meV below the conduction-band edge of P25 TiO₂.^{60,61}

According to the mechanism illustrated in Figure 2, the overall quantum efficiency for interfacial charge transfer is determined by two critical processes. They are the competition between charge-carrier recombination and trapping (picoseconds to nanoseconds) followed by the competition between trapped carrier recombination and interfacial charge transfer (microseconds to milliseconds). An increase in either the recombination lifetime of charge carriers or the interfacial electron-transfer rate constant is expected to result in higher quantum efficiencies for steady-state photolyses. This relationship is verified by time-resolved microwave conductivity studies (TRMC) of several commercial TiO₂ samples (S7–P25).^{60,61} A contour plot of the quantum efficiencies of the steady-state photolyses for the dechlorination of HCCl₃ as a function of the recombination lifetime and interfacial electron-transfer rate constant measured by TRMC is shown in Figure 3a; the subsequent linear transformation (Figure 3b) of the contour plot of Figure 3a makes the correlation more apparent. Figure 3a suggests S21–TiO₂ owes its high photoreactivity to a fast interfacial electron-transfer rate constant whereas P25 has a high photoreactivity due to slow recombination. Bickley et al.⁶³ have suggested that the anatase/rutile structure of P25 promotes charge-pair separation and inhibits recombination. The different recombination lifetimes and interfacial electron-transfer rate constants may be due to the different preparation methods of the samples that result in different crystal defect structures and surface morphologies. The correlations observed between quantum efficiencies

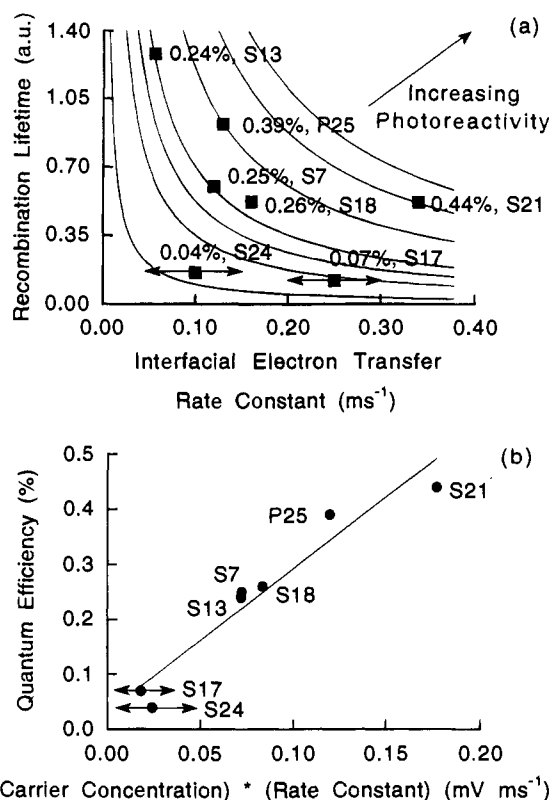


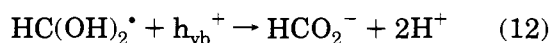
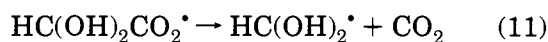
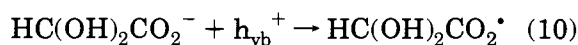
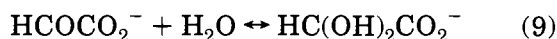
Figure 3. (a) Contour plot of quantum efficiency as a function of recombination lifetime and interfacial electron transfer rate constant and (b) linear transformation of contour plot.

and charge-carrier dynamics emphasize the importance of the interfacial charge transfer rate constant and the charge-carrier recombination lifetime as contributing factors to TiO₂ photoreactivity.

In this general mechanism, we have assumed that the substrate does not undergo direct hole transfer and that oxidative electron transfer occurs exclusively through a surface-bound hydroxyl radical, $\{>TiOH\}^+$ or equivalent trapped hole species. However, there exists a significant body of literature that oxidation may occur by either indirect oxidation via the surface-bound hydroxyl radical (i.e., a trapped hole at the particle surface) or directly via the valence-band hole before it is trapped either within the particle or at the particle surface.

In support of hydroxyl radical as the principal reactive oxidant in photoactivated TiO_2 is the observation that intermediates detected during the photocatalytic degradation of halogenated aromatic compounds are typically hydroxylated structures.^{49,64-68} These intermediates are consistent with those found when similar aromatics are reacted with a known source of hydroxyl radicals. In addition, ESR studies have verified the existence of hydroxyl and hydroperoxy radicals in aqueous solutions of illuminated TiO_2 .⁶⁹⁻⁷¹ Mao et al.⁷² have found that the rate of oxidation of chlorinated ethanes correlates with the C-H bond strengths of the organics, which indicates that H atom abstraction by OH^\bullet is an important factor in the rate-determining step for oxidation. The strong correlation between degradation rates and concentration of the organic pollutant adsorbed to the surface^{50,73-79} also implies that the hydroxyl radicals or trapped holes are directly available at the surface; however, evidence has also been presented for the homogeneous phase hydroxylation of furfuryl alcohol in aqueous ZnO suspensions.⁸⁰ On the other hand, Mao et al.⁷² have observed that trichloroacetic acid and oxalic acid are oxidized primarily by valence-band holes on TiO_2 via a photo-Kolbe process. It should be noted that these compounds also have no hydrogen atoms available for abstraction by OH^\bullet . Likewise, Draper and Fox⁸¹ were unable to find evidence of any hydroxyl radical adducts for the TiO_2 -sensitized reactions of potassium iodide, 2,4,5 trichlorophenol, tris(1,10-phenanthroline)iron(II) perchlorate; N,N,N',N' -tetramethyl-*p*-phenylenediamine, and thianthrene. In each case where the product of hydroxyl radical-mediated oxidation was known from pulse radiolysis studies to be different from that of direct electron transfer oxidation, Draper and Fox observed only the products of the direct electron-transfer oxidation.

Carraway et al.⁵¹ have provided experimental evidence for the direct hole oxidation of tightly bound electron donors such as formate, acetate, and glyoxylate at the semiconductor surface. In the case of the *gem*-diol form of glyoxylate, the photocatalytic oxidation appears to proceed via a direct hole transfer (i.e., electron transfer from the surface-bound substrate) to form formate as a primary intermediate as follows:

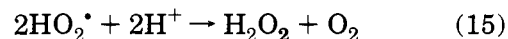
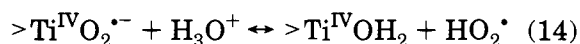
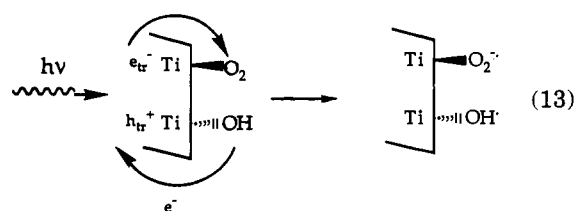


Grabner et al.⁸² have used time-resolved absorption spectroscopy to demonstrate the formation of phenoxyl and $\text{Cl}_2^{\bullet-}$ radical anions in the photooxidation of phenol on TiO_2 colloids. The formation of $\text{Cl}_2^{\bullet-}$ was postulated to occur by the direct hole oxidation of Cl^- , which was introduced into the solution as HCl to

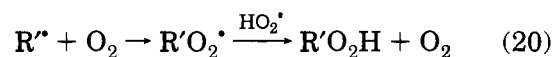
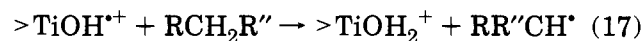
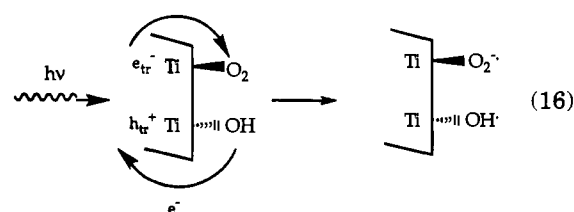
adjust the pH. Richard⁸³ has argued that both holes and hydroxyl radicals are involved in the photooxidation of 4-hydroxybenzyl alcohol (HBA) on ZnO or TiO_2 . His results suggest positive holes and hydroxyl radicals have different regioselectivities in the photocatalytic transformation of HBA. Hydroquinone (HQ) is thought to result from the direct oxidation of HBA by h_{vb}^+ , dihydroxybenzyl alcohol (DHBA) from the reaction with OH^\bullet , while 4-hydroxybenzaldehyde (HBZ) is produced by both pathways. In the presence of isopropyl alcohol (*i*-PrOH), which is used as a OH^\bullet quencher, the formation of DHBA is completely inhibited and the formation of HBZ is inhibited.

B. Formation of Reactive Oxygen Species

Hydrogen peroxide is formed on illuminated TiO_2 surfaces in the presence of air via dioxygen reduction by a conduction-band electron in the presence of a suitable electron donor such as acetate according to the following mechanism:^{51,84,85}



In the presence of organic scavengers, organic peroxides and additional H_2O_2 may be formed through the following generalized sequence:^{51,84}



where $\text{RR}''\text{CH}_2$ is a general organic electron donor with an abstractable hydrogen atom and $\text{RR}''\text{CH}^\bullet$ is the free-radical intermediate produced by oxidation of $\text{RR}''\text{CH}_2$.

In most experiments and applications with semiconductor photocatalysts, oxygen is present to act as

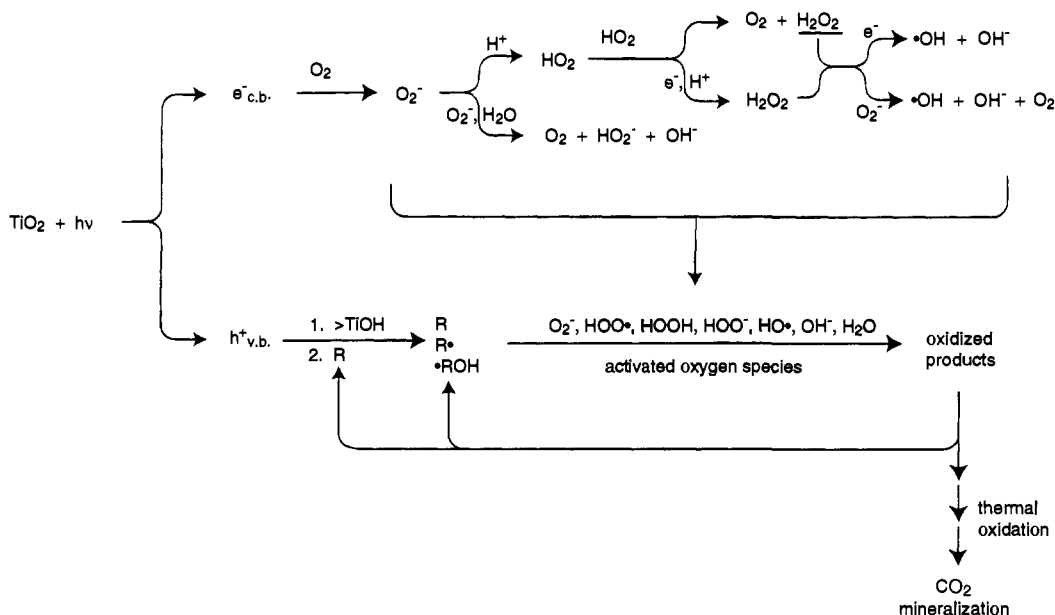
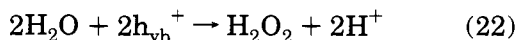
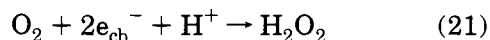


Figure 4. Secondary reactions with activated oxygen species in the photoelectrochemical mechanism.

the primary electron acceptor. As a consequence of the two-electron reduction of oxygen, H_2O_2 is formed via the above mechanism. This process is of particular interest since Gerischer and Heller have suggested that electron transfer to oxygen may be the rate-limiting step in semiconductor photocatalysis.^{43,86,87} Hydroxyl radicals are formed on the surface of TiO_2 by the reaction of h_{vb}^+ with adsorbed H_2O , hydroxide, or surface titanol groups ($>\text{TiOH}$); these processes are summarized and illustrated in Figure 4. H_2O_2 may also contribute to the degradation of organic and inorganic electron donors by acting as a direct electron acceptor or as a direct source of hydroxyl radicals due to homolytic scission. However, we need to point out that due to the redox potentials of the electron-hole pair, H_2O_2 can theoretically be formed via two different pathways in an aerated aqueous solution as follows:



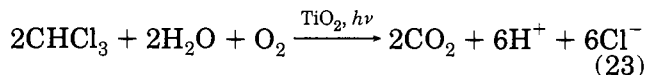
Hoffman et al.⁸⁵ and Kormann et al.⁸⁴ have shown that the quantum yield for hydrogen peroxide production during the oxidation of a variety of low molecular weight compounds has a pronounced Langmuirian (i.e., Langmuir-Hinshelwood) dependence on the O_2 partial pressure. These observations suggest that the primary formation of H_2O_2 occurs via the reduction of adsorbed oxygen by conduction band electrons. Hoffman et al.⁸⁵ have used ^{18}O isotopic labeling experiments to demonstrate that all of the oxygen in photochemically produced hydrogen peroxide (e.g., $\text{H}^{18}\text{O}^{18}\text{OH}$) arises from dioxygen (e.g., $^{18}\text{O}_2$) reduction by conduction-band electrons in the case of ZnO photocatalysis of carboxylic acid oxidation. No H_2O_2 is detected in the absence of oxygen.

III. Chemical Kinetics of Semiconductor Photocatalysis

A. Heterogeneous Photochemical Kinetics

1. Reaction Stoichiometry

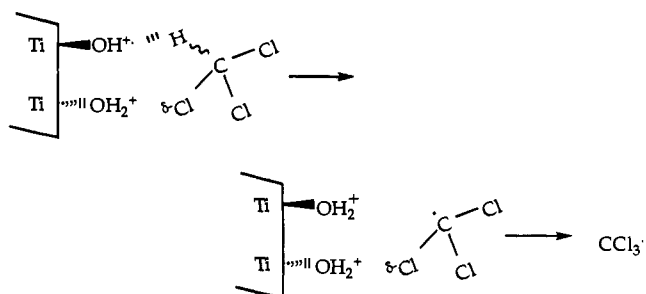
In general, the rates of change of a chemical substrate undergoing photocatalytic oxidation or reduction can be treated empirically without consideration of detailed mechanistic steps as given above. In the case of the photocatalytic oxidation of chloroform on bulk-phase TiO_2 , which occurs according to the following stoichiometry:



the rate of chloroform degradation in a well-mixed slurry reactor conforms to the following standard kinetic relationship:⁵⁰

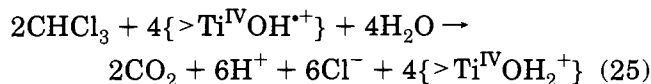
$$-\frac{d[\text{CHCl}_3]}{2dt} = -\frac{d[\text{O}_2]}{dt} = \frac{d[\text{Cl}^-]}{6dt} \quad (24)$$

An obvious consequence of the limitations imposed by the stoichiometry of eq 24 is that the extent of degradation of the substrate, in this case chloroform, will depend on the availability of oxygen as a limiting reagent, even though from a mechanistic perspective the reaction is initiated by hydrogen atom abstraction via the action of a surface-bound hydroxyl radical, $>\text{TiOH}^\bullet$ as follows:



Unless oxygen or another suitable electron acceptor (e.g., H_2O_2 , O_3 , BrO_4^- , IO_4^- , HSO_5^-) is supplied on a continuous basis to a photocatalytic reactor, the rate of photocatalytic oxidation will decrease dramatically after depletion of the primary electron acceptor due to charge-carrier recombination.

In the absence of O_2 , the principal stoichiometric oxidant will be the surface-bound hydroxyl radical, $\{\text{TiOH}^*\}^+$, with an overall stoichiometry of



The intrinsic rate of production of TiOH^+ will be limited by the photon flux and the relative efficiency of surface titanol groups as $h\nu^+$ traps. By using the mechanism of eqs 2–8, the quantum efficiency of a charge pair generated by eq 2 toward the oxidation of a substrate as indicated by eq 7 is given by

$$\phi_7 = \frac{k_7[\text{TiOH}^+][\text{Red}]}{I_a} \quad (26)$$

where the absorbed light intensity, I_a , is constant, k_7 is the rate constant of eq 7, (where the rate of eq 7 is $\nu_7 = \phi_7 I_a$), and ϕ_7 is the quantum efficiency of eq 7. During continuous irradiation over relatively short periods of time with $\lambda \leq \lambda_g$, $[h\nu^+]$, $[e_{cb}^-]$, $\{\text{Ti}^{\text{III}}\text{OH}\}$, $\{\text{TiOH}^*\}^+$, $[\text{Red}]$, and $[\text{Ox}]$ may be considered constant because changes due to the photooxidation of primary substrate (i.e., Red) occur much more slowly (minutes) than the time period of the transition from transient conditions to steady-state conditions (ms).

2. Reaction Rates, Surface Interactions, and Quantum Efficiencies

If we consider a typical set of conditions in a slurry reactor in which TiO_2 particles are suspended in solution at a nominal concentration of 0.5 g L^{-1} and we assume that each particle is spherical in shape with an average particle diameter of 30 nm and a density of 3.9 g cm^{-3} , then each discrete TiO_2 particle contains 4.16×10^5 TiO_2 molecules. On the basis of this simple calculation, the molar concentration of particles is 15 nM. At this concentration, particles of this relative size (e.g., Degussa P25) absorb light at a rate of $2.5 \times 10^{-4} \text{ mol } h\nu \text{ L}^{-1} \text{ min}^{-1}$. Given this absorbed photon flux each particle is hit by a photon on the average of every 4 ms. If $\phi_7 \approx 1$, then the maximum possible rate of substrate oxidation by surface-bound hydroxyl radicals would be

$$\nu_7 = \phi_7 I_a = 2.5 \times 10^{-4} \text{ M min}^{-1} \quad (27)$$

However, given the high probability of charge-carrier recombination (eqs 5 and 6), $\phi_7 \ll 1$ and $\nu_7 \ll 2.5 \times 10^{-4} \text{ M s}^{-1}$. Thus, we see that in the absence of O_2 or other electron acceptors, the background rate of oxidation of electron donors decreases dramatically as shown by Kormann et al.⁵⁰

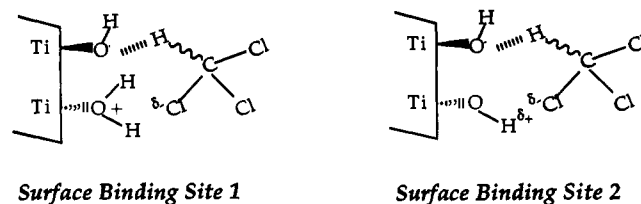
As reported by Kormann et al.,⁵⁰ typical empirical rates of degradation show the following form written here for chloroform oxidation:

$$-\frac{d[\text{CHCl}_3]}{dt} = \phi I_a [\text{O}_2]_{\text{ads}} [\text{CHCl}_3]_{\text{ads}} \quad (28)$$

in which ϕ is an effective photon-to-product conversion efficiency, I_a is the absorbed light intensity, $[\text{O}_2]_{\text{ads}}$ is the oxygen adsorbed, and $[\text{CHCl}_3]_{\text{ads}} = [\text{CHCl}_3]\Theta_{\text{CHCl}_3}$ is the chloroform adsorbed to the particles where Θ_{CHCl_3} is the fraction of chloroform adsorbed. Ollis and co-workers^{88,89} have shown that the extent of adsorption of several chlorinated hydrocarbons can be satisfactorily described in terms of a Langmuirian adsorption isotherm for a concentration range in which $[\text{CHCl}_3] < 1 \text{ mM}$. However, at higher concentrations, Kormann et al. have found it necessary to use a two-site Langmuirian model to express the observed rate of reaction for chloroform concentrations $> 1 \text{ mM}$ of the following form:

$$\theta_{\text{CHCl}_3, \text{ads}} = \frac{X_1 K_1 [\text{CHCl}_3]}{1 + K_1 [\text{CHCl}_3]} + \frac{X_2 K_2 [\text{CHCl}_3]}{1 + K_2 [\text{CHCl}_3]} \quad (29)$$

where X_1 is the fraction of total surface sites represented by the strong binding sites, X_2 is the fraction of total surface sites represented by the weak binding sites, and K_1 and K_2 are the apparent surface binding constants for CHCl_3 binding to the two different sites. In the case of chloroform interacting with Degussa P25 at pH 5, Kormann et al.⁵⁰ determined $X_1 = 2\%$, $X_2 = 98\%$, $K_1 = 10^4 \text{ M}^{-1}$, and $K_2 = 1 \text{ M}^{-1}$. At concentrations $\leq 1 \text{ mM}$ only the strong binding site (i.e., K_1) dominates sorption, while at concentrations of $\text{CHCl}_3 > 1 \text{ mM}$ most of the observed rate of reaction can be attributed to activity at the weak binding site (i.e., K_2). The two-different modes of binding can be visualized as follows:



The kinetic effect of the electron acceptor, dioxygen, on the overall rate of reaction can be modeled in terms of a simple Langmuir adsorption isotherm:

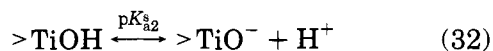
$$\theta_{\text{O}_2, \text{ads}} = \frac{K_0 [\text{O}_2]}{1 + K_0 [\text{O}_2]} \quad (30)$$

In the case of O_2 binding to Degussa P25 TiO_2 , Kormann et al.^{50,84} found a value of $K_0 = (13 \pm 7) \times 10^4 \text{ M}^{-1}$, while Mills et al.⁹⁰ reported a value of $K_0 = 3.4 \times 10^3 \text{ M}^{-1}$ for the photooxidation of 4-chlorophenol. For comparison Okamoto et al.⁹¹ reported a value of $K_0 = 8.6 \times 10^3 \text{ M}^{-1}$ for the photooxidation of phenol.

B. Surface Chemistry of Metal Oxide Semiconductors

The interactions of electron donors and electron acceptors with metal oxide semiconductors is determined, in part, by surface chemistry intrinsic to this class of compounds.⁶² Metal oxide particles sus-

pended in water are known to be amphoteric. In titration experiments, metal oxide suspensions behave as if they were simple diprotic acids.⁹²⁻⁹⁴ In the case of TiO₂, the principal amphoteric surface functionality is the "titanol" moiety, >TiOH. Hydroxyl groups on the TiO₂ surface are known to undergo the following acid-base equilibria:



where >TiOH represents the "titanol" surface group, $\text{p}K_{\text{a}1}^{\text{s}}$ is the negative log of the microscopic acidity constant for the first acid dissociation of eq 31, and $\text{p}K_{\text{a}2}^{\text{s}}$ is the negative log of the microscopic acidity constant for the second acid dissociation of eq 32. The pH of zero point of charge, pH_{zpc} , is given by one-half of the sum of the two surface $\text{p}K_{\text{a}}$'s (as in the case of amphoteric amino acids) as follows:

$$\text{pH}_{\text{zpc}} = \frac{1}{2}(\text{p}K_{\text{a}1}^{\text{s}} + \text{p}K_{\text{a}2}^{\text{s}}) \quad (33)$$

The pH_{zpc} is readily determined by titration and other experimental techniques. Due to electrostatic effects of the electrical double layer surrounding charged particles, the microscopic acidity constants need to be corrected (e.g., as in the case of activity coefficients) to yield the intrinsic surface acidity constants as follows:

$$K_{\text{a}1,\text{intr}}^{\text{s}} = K_{\text{a}1}^{\text{s}} \exp(-F\psi_0/RT) \quad (34)$$

$$K_{\text{a}2,\text{intr}}^{\text{s}} = K_{\text{a}2}^{\text{s}} \exp(-F\psi_0/RT) \quad (35)$$

where ψ_0 is the surface potential. The relationship between net surface charge, σ_p (with units of C m⁻²), and surface potential for a diffuse layer model is

$$\sigma_p = \sqrt{(8RT\epsilon\epsilon_0 C \cdot 10^3) \sinh(Z\Psi_0 F/2RT)} \quad (36)$$

where $R = 8.314 \text{ J mol}^{-1} \text{ K}^{-1}$, T is temperature (in units of K), ϵ is the dielectric constant of water (i.e., 78.5 at 298 K), ϵ_0 is the permittivity of free space (i.e., $8.854 \times 10^{-12} \text{ C}^2 \text{ J}^{-1} \text{ m}^{-1}$), C is the molar concentration of background electrolyte (M), and Z is the ionic charge for a symmetrical electrolyte. In the case of low surface potential, eq 36 can be expanded to give a linearized form as follows:

$$\sigma_p \cong \epsilon\epsilon_0 \kappa \Psi_0 \quad (37)$$

where κ is the inverse thickness of the electrical double layer (κ^{-1} is in meters) and is given by

$$\sigma_p = \sqrt{\left(\frac{2F^2\mu \cdot 10^3}{\epsilon\epsilon_0 RT}\right)} \quad (38)$$

and where μ is the ionic strength in molar units. At 298 K, $\sigma_p \cong 2.3 \mu^{1/2} \Psi_0$. For example, the thickness of the diffuse double layer, κ^{-1} , at 298 K in the presence of 3 mM NaCl as a background electrolyte is 10 nm.

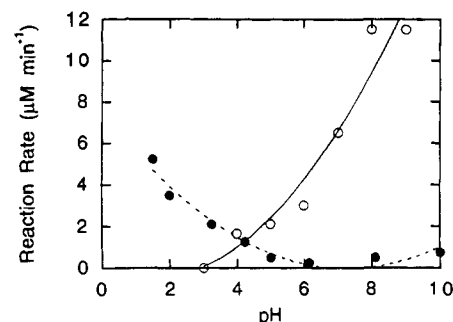
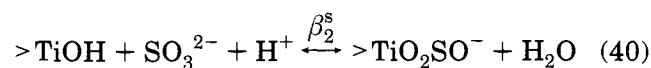
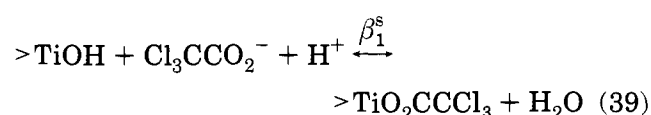


Figure 5. pH dependence of the rate of degradation of trichloroacetate (●) and chloroethylammonium (○) ions where $[\text{CCl}_3\text{CO}_2^-]_0 = [\text{Cl}(\text{CH}_2)_2\text{NH}_2]_0 = 10 \text{ mM}$, $[\text{TiO}_2] = 0.5 \text{ g L}^{-1}$, $[\text{O}_2]_0 = 0.25 \text{ mM}$, and $I_a (310\text{--}380 \text{ nm}) = 2.5 \times 10^{-4} \text{ einstein L}^{-1} \text{ min}^{-1}$.

In the case of Degussa P25, the corresponding surface acidity constants were found to be $\text{p}K_{\text{a}1}^{\text{s}} = 4.5$, $\text{p}K_{\text{a}2}^{\text{s}} = 8$ which yield a $\text{pH}_{\text{zpc}} = 6.25$.⁵⁰ The surface proton exchange capacity of P25 is 0.46 mol g^{-1} with a specific surface area of $50 \text{ m}^2 \text{ g}^{-1}$. In very simple terms, a pH_{zpc} of 6.25 for TiO₂ implies that interactions with cationic electron donors and electron acceptors will be favored for heterogeneous photocatalytic activity at high pH under conditions in which the $\text{pH} > \text{pH}_{\text{zpc}}$, while anionic electron donors and acceptors will be favored at low pH under conditions in which $\text{pH} < \text{pH}_{\text{zpc}}$.

A variety of electron-donating (e.g., Cl^- , SO_3^{2-} , HCO_2^- , CH_3CO_2^- , $\text{ClCH}_2\text{CO}_2^-$, $\text{Cl}_3\text{CCO}_2^-$, $\text{C}_6\text{H}_5\text{Cl}_3\text{-CH}_2\text{CO}_2^-$) and electron-accepting (e.g., HSO_5^- , ClO_3^- , IO_4^- , HO_2^- , OCl^- , OBr^- , $\text{S}_2\text{O}_8^{2-}$, $\text{P}_2\text{O}_8^{4-}$) substrates and nonredox ligands (e.g., HCO_3^- , CO_3^{2-} , HPO_4^-) in aqueous solution undergo inner-sphere ligand substitution reactions with the surface of TiO₂ as follows:



Kormann et al.⁵⁰ have argued that the observed enhanced rates of oxidation of many electron-donating cations at alkaline pH (i.e., $\text{pH} \gg \text{pH}_{\text{zpc}}$) cannot be explained by a simple shift of the band edges of TiO₂ in aqueous solution. If shifting the redox potential of the band edges was dominating the reactivity of the TiO₂ particles, then lower rates of substrate oxidation should be observed at high pH since the valence-band edge (i.e., the redox potential of the valence-band hole or trapped hole) decreases by 59 mV for each increasing unit of pH. Surface sorption of the electron donor to TiO₂ particles appears to play a more important role in determining the photoreactivity than shifts in nominal redox potentials of h_{vb}^+ and e_{cb}^- .

In the case of trichloroacetic acid oxidation on TiO₂ (Figure 5), the rate of reaction increases with a decrease in pH below the pH_{zpc} . This trend parallels the observed and predicted degree of inner-sphere complexation of $\text{Cl}_3\text{CCO}_2\text{H}$ by >TiOH surface sites

according to eq 39. The rate of trichloroacetic acid oxidation was near zero above the pH_{zpc} . On the other hand, in the case of the oxidation of protonated secondary amines, surface complexation is favored at pH values above the pH_{zpc} . In turn, the rate of photooxidation increases as the fraction of protonated amine present on the surface increases.

Hoffmann and co-workers^{50,94} have utilized the PC-based Fortran program SURFEQL,⁹⁵ which was developed to perform general purpose multiphase equilibrium calculations, to predict on a fundamental thermodynamic basis, the surface speciation of electron donors and electron acceptors on metal oxide semiconductors. Detailed equations and examples of the application of this code are provided by Faust et al.⁹⁴

Moser et al.⁷³ reported that monodentate and bidentate benzene derivatives, such as benzoic acid, phthalic acid, isophthalic acid, terephthalic acid, salicylic acid, and catechol were strongly bound to the surface of TiO_2 colloids. Sorption of these substrates followed a typical Langmuir isotherm. Electrophoretic measurements showed that the adsorption was accompanied by a decrease in the pH_{zpc} by 0.5 pH unit. At pH 3.6, the influence of the adsorbate on the ζ potential (ψ_z) of the TiO_2 particles is relatively small. The largest effect is observed with isophthalate, which decreases ψ_z from 78 to 51 mV. In addition, Moser et al. used laser photolysis experiments to show that surface complexation of TiO_2 by the benzene derivatives drastically accelerated the electron transfer from the conduction band of the colloidal oxide to acceptors in solution. The rate enhancement depended strongly on the structure and chemical nature of the adsorbate. At monolayer coverage, isophthalate enhances the rate of interfacial electron transfer to methylviologen (MV^{2+}) 1700 times while terephthalate increased the rate by a factor of 133-fold. Similar effects were observed for oxygen as an electron acceptor.

Tunesi et al.⁷⁷ explored the role of phenyl substituent groups in the formation of surface complexes at the surface of titanium dioxide ceramic membranes using cylindrical internal reflection-Fourier transform infrared (CIR-FTIR) spectroscopy. They did not observe any adsorption of the substrates on the rutile phase of TiO_2 , and thus they excluded the role of 5-fold coordinated Ti cations in the sorption process. For the anatase phase, they noted that single isolated carboxylate groups do not result in strong surface complexation (e.g., benzoic acid), but that amino and hydroxyl groups substituted in the ortho position to a carboxylate group (e.g., salicylic, 3-chlorosalicylic, and anthranilic acid) result in the formation of strong mononuclear bidentate surface complexes with 4-fold coordinated surface titanium cations.

Ohtani et al.⁷⁵ present a detailed mechanism for the photooxidation of alcohols on TiO_2 that requires the reductive and oxidative trapping of pairs of photoexcited electrons and holes by surface-adsorbed substrates. In the absence of appropriate substrate sorption, they report that recombination of the initial excited state is extremely rapid. Coverage of surface sites with 2-propanol via Langmuirian adsorption

was reported to control the distribution of free holes generated by the reductive trapping by surface-bound Ag^+ .

Numerous investigators have reported that the rates of photodegradation of chemical compounds on semiconductor surfaces follow the classical Langmuir-Hinshelwood expression and that the sorption of substrates to the semiconductor surfaces follows most often Langmuir sorption isotherms.^{74,96-111}

C. Langmuir-Hinshelwood Kinetics

In the Langmuir-Hinshelwood treatment of heterogeneous surface reactions, the rate of the photochemical degradation¹¹²⁻¹¹⁷ can be expressed in general terms for both the oxidant (e.g., O_2) and the reductant (e.g., CHCl_3) as follows:

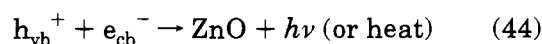
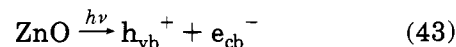
$$-\frac{d[\text{Red}]}{dt} = -\frac{d[\text{Ox}]}{dt} = k_d \theta_{\text{Red}} \theta_{\text{Ox}} \quad (41)$$

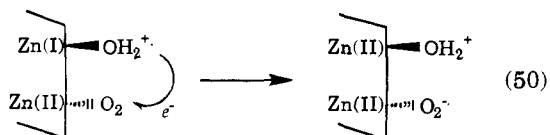
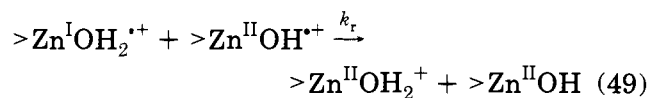
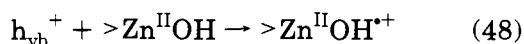
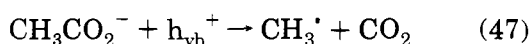
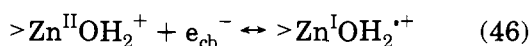
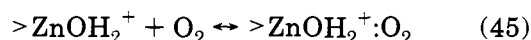
where k_d is the photodegradation rate constant, θ_{Red} represents the fraction of the electron-donating reductant (e.g., chloroform) sorbed to the surface, and θ_{Ox} represents the corresponding fraction of the electron-accepting oxidant (e.g., oxygen) sorbed to the surface. This treatment is subject to the assumptions that sorption of both the oxidant and the reductant is a rapid equilibrium process in both the forward and reverse directions and that the rate-determining step of the reaction involves both species present in a monolayer at the solid-liquid interface. The equilibrium constant, K_{ads} , for sorption of each reactant is assumed to be readily determined from a classical Langmuir sorption isotherm. In this case, the surface concentration of the reactants is related to their corresponding activities or concentrations in the bulk aqueous phase as follows:

$$\theta_{\text{Red}} = \frac{K_{\text{ads}} a_{\text{Red}}}{(1 + K_{\text{ads}} a_{\text{Red}})} = \frac{K_{\text{ads}} C_{\text{Red}} \gamma_{\text{Red}}}{(1 + K_{\text{ads}} C_{\text{Red}} \gamma_{\text{Red}})} = \frac{K'_{\text{ads}} C_{\text{Red,eq}}}{(1 + K'_{\text{ads}} C_{\text{Red,eq}})} \quad (42)$$

where a_{Red} is the equilibrium activity of the reductant in aqueous solution, γ_{Red} is the activity coefficient of the reductant, and $C_{\text{Red,eq}}$ is the equilibrium concentration of the reductant in aqueous solution. An analogous expression is also written for the oxidant as shown in eq 30 for the case of oxygen as the electron acceptor.

In order to see the kinetic basis for the empirical observations embodied in eqs 41 and 42, we can explore the photocatalyzed oxidation of acetate on ZnO particles with the corresponding reduction of dioxygen to produce hydrogen peroxide.^{84,85,93,118} In this case, we assume that acetate is sorbed at its saturation value (i.e., $\theta_{\text{CH}_3\text{CO}_2\text{H}} = 1$) and that we are looking primarily at H_2O_2 production from O_2 reduction. The proposed mechanism^{51,84,85} is as follows:





If the rate-determining step is the reduction of the adsorbed oxygen with surface-trapped electrons, then the rate of reduction of dioxygen to produce superoxide, which in turn self-reacts to produce hydrogen peroxide, is given by

$$\frac{d[\text{O}_2^{*\cdot-}]_{\text{ads}}}{dt} = k_{50} [>\text{Zn}^{\text{I}}\text{OH}_2^{*\cdot}] [>\text{Zn}^{\text{II}}\text{O}_2]_{\text{ads}} \quad (51)$$

Standard steady-state analysis on $[\text{Zn}^{\text{I}}-\text{H}_2\text{O}^{\cdot}]$ and on $[e_{\text{cb}}^-]$, under the assumption that after absorption of a single photon $[h_{\text{vb}}^+] = [e_{\text{cb}}^-]$, yields the following kinetic expression for high light intensity conditions:⁸⁵

$$\frac{d[\text{O}_2^{*\cdot-}]_{\text{ads}}}{dt} = \frac{k_{50} k_{46} k_{44}^{-1/2} I_{\text{abs}}^{1/2} [>\text{Zn}^{\text{II}}\text{OH}_2^+] [>\text{Zn}^{\text{II}}\text{O}_2]_{\text{ads}}}{k_{-46} + k_{50} [>\text{Zn}^{\text{II}}\text{O}_2]_{\text{ads}}} \quad (52)$$

and the corresponding equation for low intensity is given by

$$\frac{d[\text{O}_2^{*\cdot-}]_{\text{ads}}}{dt} = \frac{k_{50} I_{\text{abs}} [>\text{Zn}^{\text{II}}\text{O}_2]_{\text{ads}}}{k_{-46} + k_{50} [>\text{Zn}^{\text{II}}\text{O}_2]_{\text{ads}}} \quad (53)$$

Rearrangement of these equations and collection of the intrinsic rate constants gives the following simplified Langmuir–Hinshelwood-type equation for the conditions of high light intensity:

$$\frac{d[\text{O}_2^{*\cdot-}]_{\text{ads}}}{dt} = \frac{k_{\text{obs}} K' [>\text{Zn}^{\text{II}}\text{O}_2]_{\text{ads}}}{1 + K' [>\text{Zn}^{\text{II}}\text{O}_2]_{\text{ads}}} \quad (54)$$

where $k_{\text{obs}} = k_{46} k_{44}^{-1/2} I_{\text{abs}}^{1/2} [>\text{Zn}^{\text{II}}\text{OH}_2^+]$ and $K' = k_{50} / k_{-46}$ and an analogous rate expression for low light intensity

$$\frac{d[\text{O}_2^{*\cdot-}]_{\text{ads}}}{dt} = \frac{I_{\text{abs}} K' [>\text{Zn}^{\text{II}}\text{O}_2]_{\text{ads}}}{1 + K' [>\text{Zn}^{\text{II}}\text{O}_2]_{\text{ads}}} \quad (55)$$

The quantum yield for superoxide production is defined as the ratio of the rate of the reaction to the rate of photon absorption. Therefore, corresponding expressions for the quantum yields at high light

intensity and at low light intensity, respectively, are as follows:

$$\Phi = \frac{k'_{\text{obs}} I_{\text{abs}}^{-1/2} K' [>\text{Zn}^{\text{II}}\text{O}_2]_{\text{ads}}}{1 + K' [>\text{Zn}^{\text{II}}\text{O}_2]_{\text{ads}}} \quad (56)$$

$$\Phi = \frac{K' [>\text{Zn}^{\text{II}}\text{O}_2]_{\text{ads}}}{1 + K' [>\text{Zn}^{\text{II}}\text{O}_2]_{\text{ads}}} \quad (57)$$

As can be readily seen, these equations are also in the general Langmuirian form.

D. Heterogeneous Quantum Efficiencies

In photodegradation studies, the apparent quantum efficiency is often defined as the initial measured rate of photodegradation divided by the theoretical maximum rate of photon absorption (assuming that all photons are absorbed by the semiconductor and that actual light-scattering losses out of the reaction cell are negligible) as determined by chemical actinometry. This definition for species i can be expressed as follows:

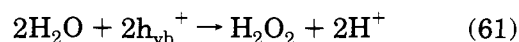
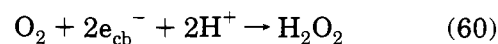
$$\Phi_{X_i} \equiv \frac{\pm(d[X_i]/dt)_0}{d[h\nu]_{\text{inc}}/dt} \quad (58)$$

where Φ_{X_i} is the apparent quantum efficiency for chemical species, X_i ; $d[X_i]/dt$ is either the initial rate of formation or loss of chemical species, X_i ; and $d[h\nu]/dt$ is the incident photon flux per unit volume.

In the case of hydrogen peroxide production coupled to acetate oxidation, a general empirical rate expression of the following form is observed:^{84,85,118}

$$\frac{d[\text{H}_2\text{O}_2]}{dt} = \Phi_0 \frac{d[h\nu]_{\text{abs}}}{dt} = f(\text{CH}_3\text{CO}_2\text{H}, \text{O}_2) = k_p \theta_{\text{CH}_3\text{CO}_2\text{H}} \theta_{\text{O}_2} \quad (59)$$

for the overall stoichiometric equations



Since hydrogen peroxide is also destroyed by reaction with holes or trapped holes on the surface, one must also consider the photochemical rate of peroxide destruction as follows:

$$-\frac{d[\text{H}_2\text{O}_2]}{dt} = \Phi_1 [\text{H}_2\text{O}_2] \frac{d[h\nu]_{\text{abs}}}{dt} = f(\text{CH}_3\text{CO}_2\text{H}, \text{O}_2, \text{H}_2\text{O}_2) \quad (62)$$

Combining the expressions for peroxide production and destruction yields an overall empirical equation of the following form:

$$\frac{d[\text{H}_2\text{O}_2]}{dt} = (\Phi_0 - \Phi_1 [\text{H}_2\text{O}_2]) \frac{d[h\nu]_{\text{abs}}}{dt} \quad (63)$$

where Φ_0 is the quantum yield for peroxide production and Φ_1 is the quantum yield for peroxide destruction at the illuminated interface. During

continuous photolysis a photostationary state is achieved which yields the very simple steady-state relationship valid for long irradiation times in a photochemical reactor:

$$[\text{H}_2\text{O}_2]_{\text{ss}} = (\Phi_0/\Phi_1) \quad (64)$$

Equation 64 states that the steady-state concentration of an intermediate, which also serves as an electron donor, in a photochemical reactor is given by the ratios of the intrinsic quantum yields for production and destruction.

E. Sorption of Electron Donors and Acceptors

From the above discussion, it is clear that sorption of electron donors and electron acceptors to the semiconductor surface is a critical step in photodegradation. The summation of chemical and electrostatic forces that bring substrates into contact with photoactive semiconductor surfaces include: inner-sphere ligand substitution (*vide supra*) for metal ions and conventional organic and inorganic ligands, van der Waals forces, induced dipole-dipole interactions, dipole-dipole interactions, hydrogen bonding, outer-sphere complexation, ion exchange, surface organic matter partitioning, sorbate hydrophobicity, and hemimicelle formation.¹¹⁹ In general, all of these surface interactions yield sorption isotherms of a Langmuirian nature. For example, ion-exchange equilibria involving organic ions at the amphoteric semiconductor surface (i.e., with both positively and negatively charged surface moieties) and in bulk aqueous solution along with competing ions will exhibit the following form:

$$[\text{organic ion}]_{\text{surface}} = \frac{K_{\text{ie}}\sigma_{\text{ie}}A[\text{organic ion}]_{\text{aq}}}{([\text{competing ion}] + [\text{organic ion}]_{\text{aq}})} \quad (65)$$

where σ_{ie} is surface charge density (mol m^{-2}), A is the specific surface area ($\text{m}^2 \text{kg}^{-1}$), and K_{ie} is the ion-exchange equilibrium constant. In Langmuirian terms, the maximum sorbed concentration is $[\text{organic ion}]_{\text{surface,max}} = \sigma_{\text{ie}}A$ and the Langmuirian equilibrium constant is $K_{\text{L}} = K_{\text{ie}}/[\text{competing ion}]$.

The hydrophobic effect, which serves to drive hydrophobic organic compounds out of the bulk aqueous phase and on to surfaces, increases regularly with the size of the nonpolar part of the molecule. For linear aliphatic organics the free energy of sorption due to hydrophobic effects can be expressed as follows:

$$\Delta G_{\text{hydrophobic}} = m \Delta G_{-\text{CH}_2-} \quad (66)$$

where m is the number of methylene groups in the aliphatic chain, and $\Delta G_{-\text{CH}_2-}$ is the hydrophobic contribution made by each methylene group to the net driving force for the organic substrate into the electrical double layer and into vicinal water. Given this consideration the charged organic substrate may be attracted to the surface by both electrostatic and hydrophobic effects. This combined effect can be expressed as follows:

$$\frac{[\text{organic}]_{\text{surf}}}{[\text{organic}]_{\text{soln}}} = \exp\left(\frac{-(\Delta G_{\text{elect}} + \Delta G_{\text{hydrophob}})}{RT}\right) = \exp\left(\frac{-(zF\psi_0 + \Delta G_{\text{hydrophob}})}{RT}\right) \quad (67)$$

IV. Bulk-Phase Semiconductors

A. Metal Oxide Semiconductors and TiO₂

Several simple oxide and sulfide semiconductors have band-gap energies sufficient for promoting or catalyzing a wide range of chemical reactions of environmental interest. They include TiO₂ ($E_{\text{g}} = 3.2$ eV), WO₃ ($E_{\text{g}} = 2.8$ eV), SrTiO₃ ($E_{\text{g}} = 3.2$ eV), α -Fe₂O₃ ($E_{\text{g}} = 3.1$ eV for $\text{O}^{2-} \rightarrow \text{Fe}^{3+}$ transitions), ZnO ($E_{\text{g}} = 3.2$ eV), and ZnS ($E_{\text{g}} = 3.6$ eV). However, among these semiconductors TiO₂ has proven to be the most suitable for widespread environmental applications. TiO₂ is biologically and chemically inert; it is stable with respect to photocorrosion and chemical corrosion; and it is inexpensive. The primary criteria for good semiconductor photocatalysts for organic compound degradation are that the redox potential of the $\text{H}_2\text{O}/\cdot\text{OH}$ ($\text{OH}^- = \cdot\text{OH} + \text{e}^-$; $E^\circ = -2.8$ V) couple lies within the bandgap domain of the material and that they are stable over prolonged periods of time. The metal sulfide semiconductors are unsuitable based on the stability requirements in that they readily undergo photoanodic corrosion, while the iron oxide polymorphs (α -Fe₂O₃, α -FeOOH, β -FeOOH, δ -FeOOH, and γ -FeOOH) are not suitable semiconductors, even though they are inexpensive and have nominally high bandgap energies, because they readily undergo photocathodic corrosion.¹²⁰

Titanium dioxide in the anatase form appears to be the most photoactive^{121,122} and the most practical of the semiconductors for widespread environmental application such as water purification, wastewater treatment, hazardous waste control, air purification, and water disinfection. ZnO appears to be a suitable alternative to TiO₂; however, ZnO is unstable with respect to incongruous dissolution^{51,85,93} to yield Zn(OH)₂ on the ZnO particle surfaces and thus leading to catalyst inactivation over time. Titanium dioxide is widely used as a white paint pigment, as a sunblocking material, as a cosmetic, and as a builder in vitamin tablets among many other uses.

In recent years, Degussa P25 TiO₂ has set the standard for photoreactivity in environmental applications, although TiO₂ produced by Sachtleben (Germany)^{60,61} and Kimera (Finland) show comparable reactivity. Degussa P25 is a nonporous 70:30% anatase-to-rutile mixture with a BET surface area of 55 ± 15 m² g⁻¹ and crystallite sizes of 30 nm in 0.1 μm diameter aggregates. Many researchers claim that rutile is a catalytically inactive^{8,90,123} or much less active form^{33,69,75,124} of TiO₂, while others find that rutile has selective activity toward certain substrates. Highly annealed ($T \geq 800$ °C) rutile appears to be photoinactive^{8,90,123} in the case of 4-chlorophenol oxidation. However, Domenech¹²⁵ has shown that TiO₂ in the rutile form is a substantially better photocatalyst for the oxidation of CN⁻ than is the anatase form; on the other hand, he also showed that Degussa P25 was a better catalyst than rutile for the photoreduction of HCrO_4^- .^{126,127}

Tanaka et al.¹²⁸ have shown that photocatalytic degradation of several compounds over different mineral phases and preparation methods of TiO₂ was dependent upon the calcination temperature for some samples and independent for others. They found that the rate of TCE photodegradation in water increased with TiO₂ calcination temperatures up to 500 °C or in some cases up to 600–700 °C and then decreased above those temperatures. They also noted that commercial anatase forms (Degussa & TP-2) were better for Cl₂CClH degradation than commercially available rutile (Katayama, TP-3 and TM-1) and that specific surface area did not appear to be a determining factor. Tanaka et al. concluded that synthesized anatase that was calcined was better than P25 and that both of these types were better than 100% rutile. However, when hydrogen peroxide was added as an electron acceptor, rutile showed greater photocatalytic activity.

Martin et al.¹²³ report an increase in photodegradation rates of 4-chlorophenol as the anatase form of TiO₂ is calcined progressively from 100 to 400 °C (i.e., the particles calcined at 400 °C yield the highest photodegradation rates) and then a decrease in photodegradation rate was noted for samples calcined above 500 °C. For comparison, the apparent quantum efficiency (eq 58) was found to be 0.23% for anatase (400 °C) and 0.03% for rutile (800 °C).

B. Metal Ion Dopants and Bulk-Phase Photoreactivity

In order to enhance interfacial charge-transfer reactions of TiO₂ bulk phase and colloidal particles, the properties of the particles have been modified by selective surface treatments such as surface chelation,^{73,129} surface derivatization,¹¹⁸ platinization,^{130,131} and selective doping of the crystalline matrix^{33,123,132–149}

Fe(III) doping of TiO₂ has been shown to increase the quantum efficiency for the photoreduction of N₂^{135,138,139} and of methyl viologen¹³⁴ and to inhibit electron–hole pair recombination,^{60,61,150} while in the case of phenol degradation, Fe(III) doping was reported to have little effect on efficiency.^{138,139} Enhanced photoreactivity for water cleavage¹⁵¹ and N₂ reduction¹³⁹ with Cr(III)-doped TiO₂ has been noted; however, others^{152,153} have found the opposite effects with Cr(III) doping. Negative effects of doping¹⁴² have been noted for Mo and V in TiO₂, while Grätzel and Howe¹³³ note an inhibition of electron–hole recombination with the same dopants. Karakitsou and Verykios³³ reported that doping TiO₂ with cations of higher valency than that of T(IV) resulted in enhanced photoreactivity, while Mu et al.¹⁵³ noted that doping with trivalent and pentavalent cations was actually detrimental to the photoreactivity of TiO₂.

Mixed-phase Ti/Fe metal oxide colloids¹⁵⁴ containing from 0.1 to 50 atom % Fe have been investigated with respect to providing a broader range of wavelengths suitable for bandgap excitation than pure TiO₂. In this regard, Bahnemann and co-workers¹⁵⁴ have studied the photodegradation of dichloroacetic acid (DCA) using Ti/Fe mixed-oxide particles with variable iron content over a broad range of pH. At

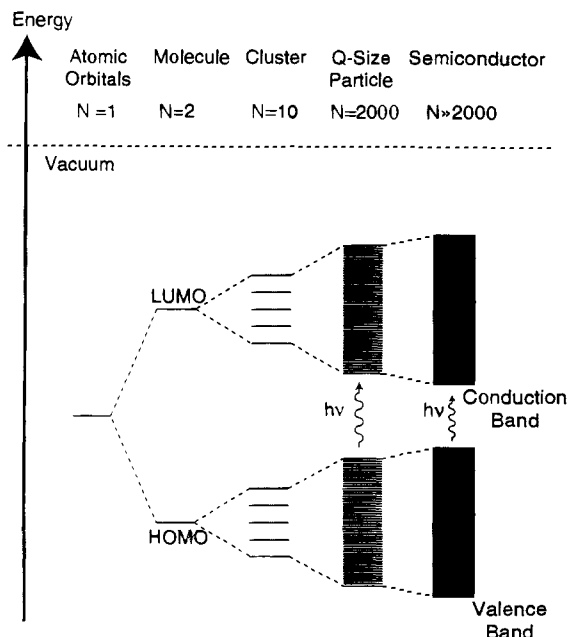


Figure 6. MO model for particle growth for N monomeric units. The spacing of the energy levels (i.e., density states) varies among systems.

pH = 2.6, they reported that the iron-containing TiO₂ particles showed higher quantum yields than pure TiO₂ colloids, although the highest enhancement in photoreactivity was obtained with an iron content of 2.5 atom %. In the latter case, the degradation of DCA was found to be almost 4 times as efficient as with pure TiO₂ colloids. Ferric ions within the TiO₂ matrix are thought to inhibit the recombination of photogenerated charge carriers. At pH = 11.3, the quantum yields for the destruction of dichloroacetic acid were found to be smaller than at pH = 2.3 due to the less favorable sorption of DCA at high pH. In addition, the energy levels of the band edges are shifted cathodically with increasing pH (59 mV per pH unit at 300 K); this shift results in a decrease of the oxidation potential of the valence-band holes at high pH and could contribute to the lower rates of DCA oxidation at pH 11.3.

V. Quantum-Sized Semiconductors

A. Basic Characteristics and Behavior

When the crystallite dimension of a semiconductor particle falls below a critical radius of approximately 10 nm, the charge carriers appear to behave quantum mechanically^{9,155–165} as a simple particle in a box (Figure 6). As a result of this confinement, the band gap increases and the band edges shift (Figure 7) to yield larger redox potentials. The solvent reorganization free energy for charge transfer to a substrate, however, remains unchanged. The increased driving force and the unchanged solvent reorganization free energy in size-quantized systems are expected to increase the rate constant of charge transfer in the normal Marcus region.^{166–168} Thus, the use of size-quantized semiconductor TiO₂ particles may result in increased photoefficiencies for systems in which the rate-limiting step is charge transfer.^{169,170}

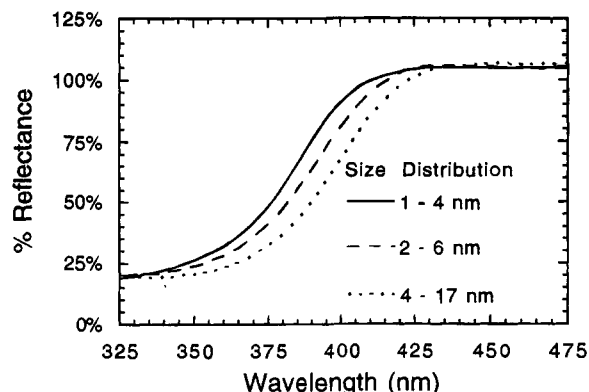


Figure 7. UV/vis reflectance spectra of size-quantized TiO_2 .

The use of size-quantized semiconductors^{85,169-173} to increase photoefficiencies is supported by several studies. However, in other work, size-quantized semiconductors have been found to be less photoactive than their bulk-phase counterparts.^{170,174} In the latter cases, surface speciation and surface defect density appear to control photoreactivity.^{94,122,175} The positive effects of increased overpotentials (i.e., difference between E_{vb} and E_{redox}) on quantum yields can be offset by unfavorable surface speciation and surface defects due to the preparation method of size-quantized semiconductor particles.

B. Doped Quantum-Sized TiO_2

Choi et al.^{150,176,177} have recently shown that selectively doped quantum- (Q-) sized particles have a much greater photoreactivity as measured by their quantum efficiencies for oxidation and reduction than their undoped counterparts. They present the results of a systematic study of the effects of 21 different metal ion dopants on the photochemical reactivity of quantum-sized TiO_2 with respect to both chloroform

oxidation and carbon tetrachloride reduction (Figure 8). Their results are summarized in terms of a periodic chart of dopant effects on oxidation and reduction quantum yields. Enhanced photoactivity was seen for Fe(III), Mo(V), Ru(III), Os(III), Re(V), V(IV), and Rh(III) substitution for Ti(IV) at the 0.5 atom % level in the TiO_2 matrix. The maximum enhancements were 18-fold (CCl_4 reduction) and 15-fold (CHCl_3 oxidation) increases in quantum efficiency for Fe(III)-doped Q- TiO_2 .

Choi et al.¹⁵⁰ used laser flash photolysis measurements to show that the lifetime of the blue electron in the Fe(III)-, V(IV)-, Mo(V)-, and Ru(III)-doped samples was increased to 50 ms, while the measured lifetimes of the blue electron in undoped Q-particles were $< 200 \mu\text{s}$.^{150,176,177} They established that the experimental quantum efficiencies for oxidation and for reduction could be correlated to the measured transient absorption signals of the charge carriers. In general, a relative increase in the concentration of the long-lived (ms) charge carriers results in a corresponding increase in photoreactivity. However, if an electron is trapped in a deep trapping site, it will have a longer lifetime but it may also have a lower redox potential that could result in a decrease in photoreactivity. Reactivity of doped TiO_2 appears to be a complex function of the dopant concentration, the energy level of the dopants within the TiO_2 lattice, their d-electronic configuration, the distribution of dopants, the electron-donor concentration, and the light intensity.

The photophysical mechanisms of doped TiO_2 are not well understood. Key questions include the following: (1) Are the transition metal ions located primarily on the surface or in the lattice? (2) Is the surficial binding of substrates affected by doping? (3) Do transition metal ions influence charge-pair recombination? (4) Do altered interfacial transfer rate

Photocatalytic Effects of Various Metal-Ion Dopants in Q- TiO_2

Li ⁺ 0.15 <0.08		Mg ²⁺		V ³⁺		V ⁵⁺		Al ³⁺ 0.08 <0.08	
		0.14 <0.08	1.02 1.72	0.51 0.66					
		upper number Φ_{CHCl_3} (%)		lower number $\Phi_{\text{CCl}_4/\text{Cl}^-}$ (%)					
Ti ⁴⁺	V ⁴⁺	Cr ³⁺	Mn ³⁺	Fe ³⁺	Co ³⁺	Ni ²⁺	Zn ²⁺	Ga ³⁺	
0.16 <0.08	1.09 1.60	0.21 0.16	0.59 0.12	2.38 1.74	0.08 <0.08	0.50 0.09	0.20 <0.08	0.15 <0.08	
Zr ⁴⁺	Nb ⁵⁺	Mo ⁵⁺		Ru ³⁺	Rh ³⁺				Sn ⁴⁺
0.09 0.11	0.23 <0.08	1.82 1.59		1.72 0.38	0.87 0.44				0.11 <0.08
	Ta ⁵⁺		Re ⁵⁺	Os ³⁺					Sb ⁵⁺
	0.27 <0.08		1.20 0.80	1.60 0.84					<0.08

All dopant concentrations are 0.5 atom% except Mo⁵⁺ (0.1 %).

Figure 8. Periodic chart of the photocatalytic effects of various metal ion dopants in TiO_2 . The upper bold-faced numbers are the quantum yields (%) for the oxidative chloroform degradation, Φ_{CHCl_3} , and the lower numbers are the quantum yields (%) for Cl^- production from the reductive dechlorination of carbon tetrachloride, $\Phi_{\text{CCl}_4/\text{Cl}^-}$. All the oxidation states represent those of the precursor metal ions. All dopant concentrations are 0.5 atom % except Mo⁵⁺ (0.1 atom %). Ti⁴⁺ refers to the undoped TiO_2 .

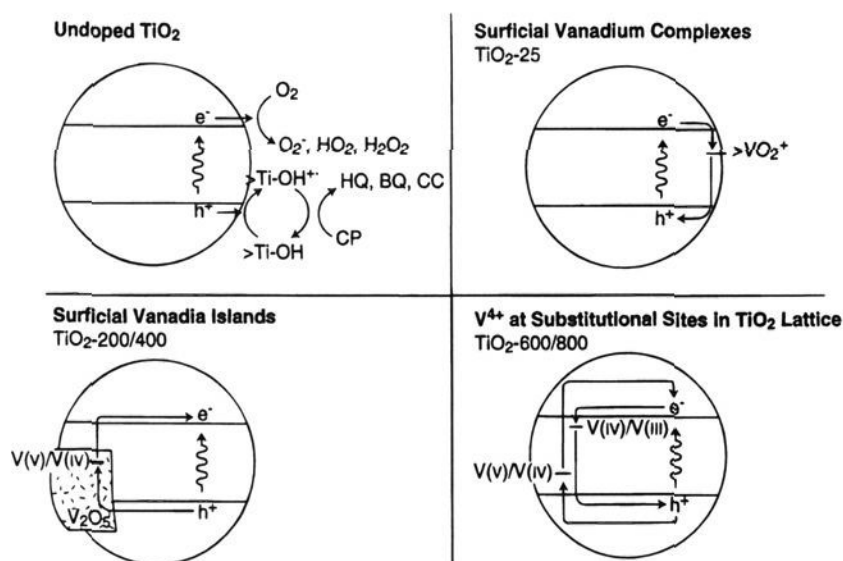


Figure 9. Charge-carrier dynamics of vanadium-doped TiO_2 .

constants associated with surficial transition metal ion complexes play a primary role in altered photochemical kinetics?

In order to address these questions, Martin et al.¹²³ selected a single dopant (vanadium) for detailed investigation to elucidate the mechanism of the dopant action on the photoreactivity of TiO_2 .¹²³ Vanadium-doped TiO_2 was prepared by standard coprecipitation methods. Five fractions were heat-treated in quartz boats for 4 h at 25, 200, 400, 600, and 800 °C and labeled TiO_2 -25 through TiO_2 -800, respectively. Vanadium doping of the crystals is found to reduce the photooxidation rates of 4-chlorophenol (4-CP) relative to undoped TiO_2 . Vanadium is present on TiO_2 -25 primarily as $>\text{VO}_2^+$ (~90%) and secondarily as interstitial V^{4+} (~10%). The deposition of vanadium as surficial islands of V_2O_5 occurs on TiO_2 -200/400. A small fraction of the total vanadium (~1%) in TiO_2 -200/400 is also present as V(IV) . Vanadium dopants in TiO_2 -600/800 are found to be present primarily as a solid solution of $\text{V}_x\text{Ti}_{1-x}\text{O}_2$.

Vanadium appears to reduce the photoreactivity of TiO_2 -25 by promoting charge-carrier recombination via electron trapping at surficial $>\text{VO}_2^+$ sites, whereas V(IV) impurities in surficial V_2O_5 islands on TiO_2 -200/400 promote charge-carrier recombination by hole trapping. Substitutional V(IV) in the lattice of TiO_2 -600/800 appears to act primarily as a charge-carrier recombination center that shunts charge carriers away from the solid-solution interface with a net reduction in photoreactivity. Figure 9 gives a pictorial view of the important electronic processes that may be operative due to vanadium doping. The energy levels of the vanadium groups are approximated based upon $\text{VO}_2^+/\text{VO}_2^{2+}$ ($E^\circ_{1/2} = +1.00$ V), $\text{VO}_2^{2+}/\text{V(III)}$ ($E^\circ_{1/2} = +0.337$ V), and bulk V_2O_5 ($E_{\text{cb}} = +0.9$ V, $E_{\text{vb}} = +3.7$ V).¹⁷⁸ The complexities of the physical and electronic effects of vanadium doping may be expected to be present in the mechanisms of other transition metal ions doped into TiO_2 (Figure 9).

VI. Photochemical Reactors

A. Water Treatment Systems

A variety of photochemical reactor configurations have been employed in photodegradation studies and for actual treatment situations (see Figure 10 for

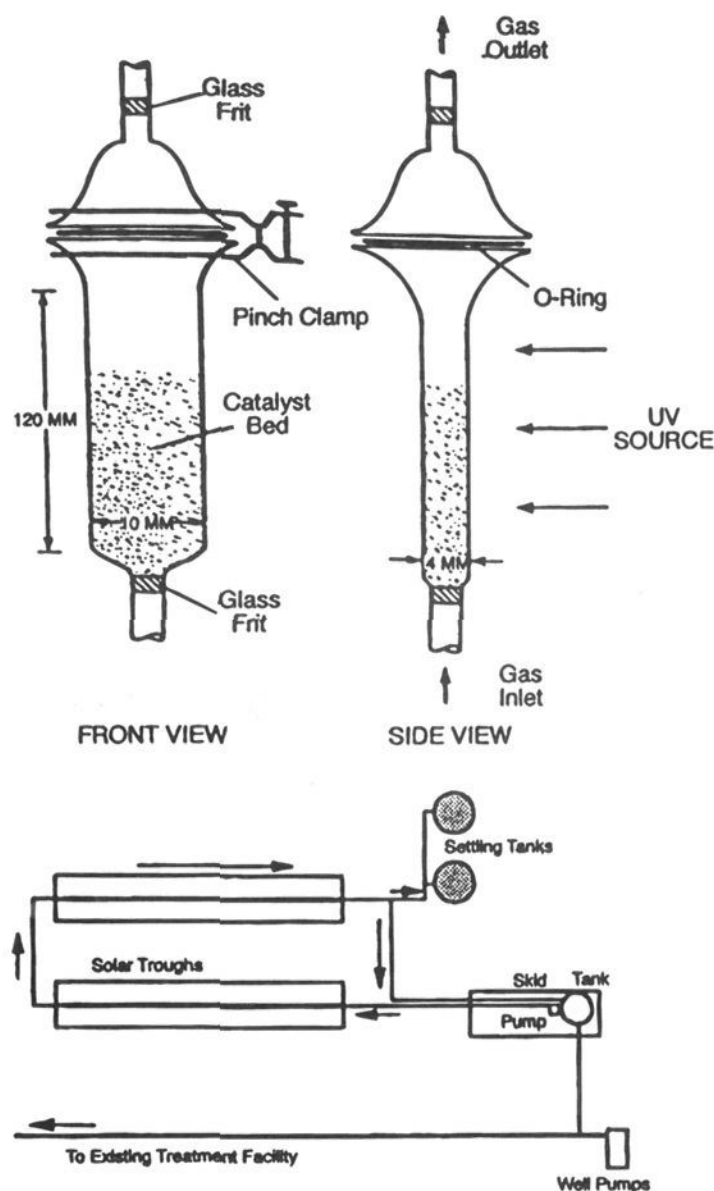
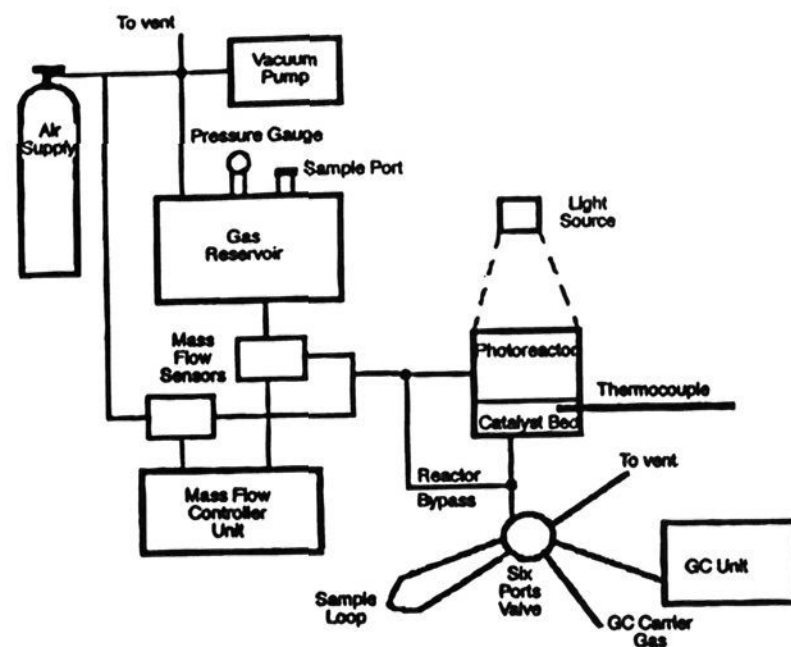


Figure 10. Photochemical reactor configurations: (a) fixed-bed continuous flow gas reactor (reprinted from Peral, J.; Ollis, D. J. *Catal.* **1992**, *136*, 554–565; copyright 1992 Academic); (b) fluidized-bed continuous flow gas reactor (reprinted from Dibble, L. A.; Raupp, G. B. *Environ. Sci. Technol.* **1992**, *26*, 492–495; copyright 1992 American Chemical Society); and (c) pilot-scale solar photocatalytic water detoxification system (reprinted from Pacheco, J. E.; Mehos, M.; Turchi, C.; Link, H. In *Photocatalytic Purification and Treatment of Water and Air*; Ollis, D. F., Al-Ekabi, H., Eds.; Elsevier Science Publishers, 1993; copyright 1993 Elsevier Science Publishers).

some examples). Most often in laboratory experiments, well-mixed heterogeneous batch reactors^{8,49–51,85,94,118,169,170,179–184} have been employed. In slurry reactors, the semiconductor particles must be separated from the bulk fluid phase after treatment by filtration, centrifugation, or coagulation and

flocculation. These added steps add various levels of complexity to an overall treatment process and they clearly decrease the economical viability of slurry reactors. Alternative reactor configurations^{28,104,110,182,183,185-202} include either fluidized^{181,203} or fixed-bed reactors.²⁰⁴ In most practical applications of semiconductor photocatalysis, fixed-bed reactor configurations with immobilized particles or semiconductor ceramic membranes may be required. A fixed-bed reactor system allows for the continuous use of the photocatalysts for processing of aqueous- or gas-phase effluents while eliminating the need for post-process filtration coupled with particle recovery and catalyst regeneration. In typical fixed-bed photocatalytic reactors the photocatalyst is coated on the walls of the reactor,^{205,206} on a solid-supported matrix, or around the casing of the light source. However, these reactors have several drawbacks; most notable are the low surface area-to-volume ratios and inefficiencies introduced by absorption and scattering of light by the reaction medium. Fine particle entrapment can be achieved by immobilization on glass beads,²⁰⁷ immobilization on walls of reaction vessels^{26,208} or tubes,^{32,209,210} immobilization on fiberglass^{211,212} or woven fibers,²¹³ and compression of fine particles into ceramic membranes.²¹⁴⁻²¹⁶

B. Gas-Phase Treatment Systems

A number of reactors have been designed specifically for the treatment of gas-phase chemical contaminants.^{32,78,199,217-225} For example, Anderson and co-workers¹⁹⁹ have developed a photochemical reactor for purification of gas streams contaminated with chlorinated hydrocarbons. They examined the photoassisted catalytic degradation of trichloroethylene (TCE) in the gas phase using a packed bed reactor containing TiO₂ pellets which were 0.3–1.6 mm in diameter. The pellets had measured porosities of 50–56% and specific surface areas of 160–194 m² g⁻¹. The apparent quantum yields for the conversion of TCE were reported to be in the range 0.4–0.9. For a single pass at a volumetric flow rate of 300 mL min⁻¹, the TCE concentration was reduced from 460 ppm in the influent stream to 3 ppm in the effluent stream (i.e., a 99.3% conversion efficiency) using only four 4 W black lights and 0.56 g of TiO₂.

Nimlos et al.²¹⁸ have also described a detailed investigation of the gas-phase photocatalytic oxidation of TCE over TiO₂. They reported very high levels of destruction of TCE in short periods of time with apparent quantum yields near 1.0. However, they used direct-sampling mass spectrometry and gas-phase Fourier transform infrared (FTIR) spectroscopy to detect significant levels of phosgene, dichloroacetyl chloride (DCAC), carbon monoxide, and molecular chlorine in the gas-phase effluent stream. Nimlos et al. present a reaction mechanism in which the TCE molecules are oxidized in a chain reaction involving Cl atoms on the hydrated surface of TiO₂ to produce DCAC as a reaction intermediate. Phosgene appears to arise from the photocatalytic oxidation of DCAC, and molecular chlorine arises from the recombination of chlorine atoms.

Phillips and Raupp⁷⁸ used transmission infrared spectra of untreated titania to show that the surface

is highly hydrated in a fixed-bed gas-scrubbing reactor designed for TCE oxidation. The IR spectra showed that nominally dry TiO₂ contains both hydroxyl groups and chemisorbed water; however, no evidence of chemisorbed trichloroethylene (TCE) was apparent in the IR spectra. They reported that illumination with UV light in the presence of TCE vapor leads to the desorption of molecular water and subsequent formation of several adsorbed intermediates (e.g., dichlorinated olefins and dichloroacetaldehyde) and carbon dioxide. Phillips and Raupp⁷⁸ compared the O–H stretching regions of the IR spectra during illumination in the absence and presence of TCE to show that surficial hydroxyl groups are consumed during TCE oxidation. Their observations are consistent with a mechanism in which water desorption is a prerequisite “trigger” step for oxygen adsorption and subsequent reactive hydroxyl radical and hydroperoxide radical formation in gas–solid reactors, as well as for TCE adsorption. They also suggested that attack of adsorbed olefinic derivatives of TCE by hydroxyl radicals or by hydroperoxide radicals leads to production of dichloroacetaldehyde. Ultraviolet illumination appeared to promote the desorption of CO₂ formed by further hydroxyl radical attack on the aldehyde intermediates.

VII. Important Reaction Variables

In addition to the particular mineral phase, the surface modifications, and the doping level of the semiconductors, other extensive and intensive reaction/reactor variables are important in determining the rate and extent of compound transformation in both aqueous- and gas-phase systems.⁸ They include the semiconductor concentration,^{49,50,84,85,94,118,170} reactive surface area,^{33,124,226-228} porosity of aggregates,^{76,123,228,229} the concentration of electron donors and acceptors,^{49,50,74,85,94,99,169,170,198,230-232} the incident light intensity,^{50,85,109,169,170,193,229,230,233-235} the pH,^{49,50,58,76,94,103,124,126,236-238} the presence of competitive sorbates,^{50,96,97,193,230,232,239-241} and the temperature.^{103,109,186}

In terms of future applications of semiconductor photocatalysis, a major concern has to be the nonlinear (e.g., photochemical rate $\propto \sqrt{I}$ or as shown in eq 56 $\Phi \propto (\sqrt{I})^{-1}$) dependence of rate (or quantum efficiency) on light intensity for many degradation reactions.^{8,17,49,50,85,112,170,229,239,242,243} This feature argues against employing concentrating solar collectors with enhanced light fluxes. The net effect would be to lower the overall efficiency of the process.

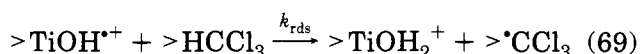
Kormann et al.⁵⁰ and Martin et al.⁶⁰ have shown that the rate of chloroform, CHCl₃, degradation in the presence of O₂ is a nonlinear function of the light intensity. The rate of reaction conformed to the following empirical expression:

$$-\frac{d[\text{CHCl}_3]}{dt} = k_{\text{obs}}\sqrt{I_a} \quad (68)$$

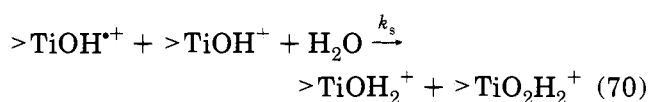
where I_a is the incident light intensity (in $\mu\text{E L}^{-1} \text{min}^{-1}$) and k_{obs} is the observed rate constant with units of $(\mu\text{E L}^{-1} \text{min}^{-1})^{1/2}$. In addition, the measured quantum yield of the reaction increases with decreas-

ing light intensity. For example, single wavelength irradiation at $\lambda = 330$ nm with an absorbed light intensity of $2.8 \mu\text{E L}^{-1} \text{min}^{-1}$ yielded $\Phi = 0.56$ for CHCl_3 degradation. On the other hand, with the absorbed light intensity increased to $250 \mu\text{E L}^{-1} \text{min}^{-1}$ under the same conditions, Φ was reduced to 0.02. Similar results have been reported by Hoffman et al.¹⁷⁰ for the photocatalytic production of poly(methyl methacrylate) via ZnO photocatalysis and by Harvey and Rudham²⁴⁴ for the photocatalytic oxidation of I^- .

As shown in development of eqs 51–57, the square-root dependence of the reaction rate can arise from enhanced bandgap recombination at higher light intensities.^{60,61,245} An alternative explanation⁵⁰ for the square-root dependence of the rate of reaction on the light intensity focuses on the role of surface-bound hydroxyl radical, $\{>\text{TiOH}^*\}^+$, as the principal hole trap and the primary initiator of oxidation of electron-donating substrates. In this mechanism it is assumed that the photogenerated conduction-band electrons are efficiently removed by an electron acceptor and that holes are trapped in relatively long-lived hole traps. The surface-bound hydroxyl radicals are thus free to initiate the oxidation of chloroform as follows:



where the symbol $>$ indicates surface-bound species. The steps after the rate-determining step are given below (*vide infra*). The rate constant k_{rds} can be estimated to be comparable to the rate constant measured for hydroxyl radical reacting with chloroform in homogeneous aqueous solution (e.g., $k = 10^7 \text{ M}^{-1} \text{ s}^{-1}$). In addition to direct H-atom abstraction from a bound substrate, the surface-bound hydroxyl radical, $\{>\text{TiOH}^*\}^+$, could in turn react with itself as follows:



provided that they are within reasonable proximity of each other on the surface. Assuming a photostationary state for $>\text{TiOH}^{*+}$ we can perform a standard steady-state kinetic analysis to obtain a quantum yield of chloroform degradation, Φ_r , that can be expressed in terms of k_{rds} and k_s as follows:

$$\frac{d[>\text{TiOH}^*]}{dt} = I_a \Phi_{>\text{TiOH}^*} - k_{\text{rds}}[>\text{TiOH}^{*+}][>\text{HCCl}_3] - k_s[>\text{TiOH}^{*+}]^2 \quad (71)$$

$$\Phi_r = \frac{k_{\text{rds}}[>\text{TiOH}^{*+}][>\text{HCCl}_3]}{k_{\text{rds}}[>\text{TiOH}^{*+}][>\text{HCCl}_3] + k_s[>\text{TiOH}^{*+}]^2} \quad (72)$$

under the assumption that the quantum yield for $>\text{TiOH}^{*+}$ production ≈ 1 . Two limiting cases for eq 72 arise. For conditions of low absorbed light inten-

sity where $k_{\text{rds}}[>\text{TiOH}^{*+}][>\text{HCCl}_3] \gg k_s[>\text{TiOH}^{*+}]^2$, $\Phi_r \rightarrow 1$ and for conditions of high absorbed light intensity, I_a , $k_s[>\text{TiOH}^{*+}]^2 \gg k_{\text{rds}}[>\text{TiOH}^{*+}][>\text{HCCl}_3]$, the overall quantum yield for the reaction is given by

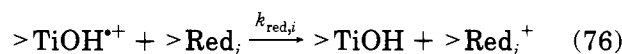
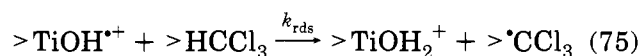
$$\Phi_r = \frac{k_{\text{rds}}[>\text{HCCl}_3]}{\sqrt{k_s I_a}} \quad (73)$$

For the oxidation of chloroform as reported by Kormann et al., a value for the ratio of rate constants is obtained as follows:

$$k_{\text{obs}} = \frac{k_{\text{rds}}}{\sqrt{k_s}} = 2.0 \times 10^{-3} (\text{M s})^{-1/2} \quad (74)$$

From the numerical value of k_{obs} we can conclude that the reaction of $>\text{TiOH}^{*+}$ with $>\text{HCCl}_3$ (k_{rds}) is relatively slow compared to an efficient second-order (k_s) recombination process with a characteristic time of 0.1 μs .

Inhibition of chlorinated hydrocarbon oxidation on irradiated TiO_2 by cations, anions, and neutral molecules can result from competition either for reactive surface sites (e.g., $>\text{TiOH}$, $>\text{TiO}^-$, and $>\text{TiOH}_2^+$) or for highly reactive transient species (e.g., $>\text{TiOH}^{*+}$) on the surface.⁵⁰ The effects of competitive electron transfer or H atom abstraction substrates on the net reaction rate of a chlorinated hydrocarbon such as HCCl_3 can be modeled in terms of a simple mechanism as follows:



where Red_i is a competitive electron donor that reacts with the surface-bound hydroxyl radical with a second-order rate constant, $k_{\text{red},i}$. The reaction of eq 76 competes effectively for $>\text{TiOH}^{*+}$ and reduces its rate of reaction with the primary electron donor (e.g., HCCl_3). Thus, the higher the concentration of competitive electron donors on the TiO_2 surface during irradiation, the more extensive the observed competitive inhibition. Given the competition for the principal oxidation initiator, $>\text{TiOH}^{*+}$, we can write an overall kinetic equation for the rate of surface hydroxyl radical production as

$$\frac{d[>\text{TiOH}^{*+}]}{dt} = I_a \Phi_{>\text{TiOH}^{*+}} - k_{\text{rds}}[>\text{TiOH}^{*+}][>\text{HCCl}_3] - k_s[>\text{TiOH}^{*+}] \sum_{i=1}^n k_{\text{red},i}[\text{Red}_i] \quad (77)$$

Under steady-state illumination we can use eq 77 to obtain the following overall rate equation for chloroform oxidation for conditions of low light intensity:

$$\frac{d[\text{HCCl}_3]}{dt} = \frac{k_{\text{rds}} I_a \Phi_{>\text{TiOH}^+} [\text{HCCl}_3]}{k_{\text{rds}} [>\text{HCCl}_3] + k_{\text{s}} [>\text{TiOH}^{*+}] \sum_{i=1}^n k_{\text{red},i} [\text{Red}_i]} \quad (78)$$

(Equation 79 deleted in proof)

VIII. Photochemical Transformation of Specific Compounds

A. Inorganic Compounds

In addition to organic compounds, a wide variety of inorganic compounds are sensitive to photochemical transformation on semiconductor surfaces. Examples include ammonia,^{96,246,247} azide,²⁴⁸ chromium species,^{214,249–251} copper,^{98,126,235,252–255} cyanide,^{96,124,126,191,197,256–262} gold,^{38,57,58,263–266} halide ions,^{81,267–269} iron species,^{98,120} manganese species,^{98,103} mercury,^{251,270,271} nitrates and nitrites,^{105,106,111,246,258,272} nitric oxide and nitrogen dioxide,^{220,247,273–276} nitrogen,^{135,277} oxygen,^{84,85,93,118,278} ozone,^{279,280} palladium species,⁵⁹ platinum species,^{59,251,281,282} rhodium species,⁵⁹ silver,^{38,75,226,251,272,279,283,284} and sulfur species^{94,106,118,179,261,285–289} among others.

In addition to the oxidative transformation of inorganic compounds, illuminated aqueous suspensions of semiconductors (CdS, CdSe, $\alpha\text{-Fe}_2\text{O}_3$, TiO_2 , and ZnO) have been shown to generate significant concentrations of hydrogen peroxide via reductive pathways.^{84,118,290–294} Hoffman et al.⁸⁵ have recently shown that ZnO produces H_2O_2 more efficiently than TiO_2 . This characteristic, combined with the relatively benign environmental effects of ZnO, may make semiconductor photocatalysis an attractive potential source of H_2O_2 production to be applied for contaminant destruction technologies.

B. Organic Compounds

Photocatalytic oxidation of organic compounds is of considerable interest for environmental applications and in particular for the control and eventual destruction (i.e., elimination) of hazardous wastes. The complete mineralization (i.e., oxidation of organic compounds to CO_2 , H_2O , and associated inorganic components such as HCl, HBr, SO_4^{2-} , NO_3^- , etc.) of a variety of aliphatic and aromatic chlorinated hydrocarbons via heterogeneous photooxidation on TiO_2 has been reported.

The general classes^{6–8,15,181,295} of compounds that have been degraded, although not necessarily completely mineralized by semiconductor photocatalysis include alkanes, haloalkanes, aliphatic alcohols, carboxylic acids, alkenes, aromatics, haloaromatics, polymers, surfactants, herbicides, pesticides, and dyes. A partial tabulation of organic reactions catalyzed by illuminated semiconductors is provided in Tables 1–4. In addition to providing these primary references, we have summarized some representative kinetic data for the photochemical oxidation of phenol and 4-chlorophenol (Table 5) that are analyzed in terms of Langmuir–Hinshelwood parameters.

Table 1. Semiconductor Photodegradation of Chlorinated Aromatics

substrate	refs
2-chlorophenol	53,54,225,302,307–313
3-chlorophenol	54,308,309,313
4-chlorophenol	8,53,76,79,90,107,112,180,186,192,198,306,308,309,311,313–325
2,4-dichlorophenol	102,306,313,320,321
3,4-dichlorophenol	53
2,6-dichlorophenol	53
2,4,5-trichlorophenol	53,81,306,313,322
pentachlorophenol	49,313,320,323–325
chlorobenzene	65,225,311,325–327
1,2,4-trichlorobenzene	328
1,3-dichlorobenzene	328
1,2-dichlorobenzene	328
1,4-dichlorobenzene	149,175,238,264
2,3,4-trichlorobiphenyl	215,329–331
2,7-dichlorodibenzo- <i>p</i> -dioxin	302,307,330,331
2-chlorodibenzo- <i>p</i> -dioxin	330,331
2,4,5-trichlorophenoxyacetic acid	322
2,4-dichlorophenoxyacetic acid	237
hexachlorobenzene	325
PCB's	215,331,332
DDT	325,333
chlorinated surfactants	55,334

Table 2. Semiconductor Photodegradation of Chlorinated Aliphatic and Olefinic Compounds

substrate	refs
1,1,1-trichloroethane	72,225
1,1,2,2-tetrachloroethane	72,325
1,1,1,2-tetrachloroethane	232
1,1,2-trichloroethane	72
1,1,2-trichloro-1,2,2-trifluoroethane	72
1,1,1-trifluoro-2,2,2-trichloroethane	325
1,1-difluoro-1,2,2-trichloroethane	325
1,1-difluoro-1,2-dichloroethane	325
1,1-dichloroethane	72
1,2-dichloroethane	65,72,311
1,2-dichloroethylene	325
1,2-dichloropropane	325
bis(2-chloroethyl) ether	325
carbon tetrachloride	65,88,118,325,335–338
chloroacetic acid	51,52,65,190,294,339–342
chloroethane	72
chloroform	50,65,88,196,225,325,326,338,343–346
methylene chloride	65,88,311,325,347,348
tetrachloroethylene	66,190,341,348–350
trichloroethylene	65,78,89,189,190,194,199,217,218,221,223,225,311,321,325,341,342,345,349,351–353
chloral hydrate	354
chloranil	49
chloroethylammonium chloride	50
dichloroacetic acid	26,52,65,205
trichloroacetic acid	50–52,65,72,120

The Langmuir adsorption constants, K_{ads} , which can be determined independently from dark adsorption isotherms, have been reported to be significantly different from the equivalent constants determined from kinetic data obtained in photocatalytic systems. Mills and Morris¹⁰⁷ have shown that the Langmuir adsorption constant for 4-chlorophenol sorbed to TiO_2 was about 200 times less than its counterpart in a TiO_2 -sensitized photodegradation system. Cunningham and Al-Sayyed²⁹⁶ have tried to predict the rates of photodegradation of substituted benzoic acids on

Table 3. Semiconductor Photodegradation of Nitrogenous Compounds

substrate	refs
2-, 3-, and 4-nitrophenol	210,236,355-358
2,5-dinitrophenol	355
trinitrophenol	355
atrazine	56,185,195,240,302, 307,356,359-362
dimethylformamide	225
nitrobenzene	56,210,237,251,309, 311,326
4-nitrophenyl ethylphenylphosphinate	305
4-nitrophenyl diethyl phosphate	305
4-nitrophenyl isopropylphenylphosphinate	305
azobenzenes	363-366
cyclophosphamide	356
EDTA	251,325,356
methyl orange	289,367-369
methylene blue	289,369,370
methyl viologen	76,81,132,207,231, 371-373
monuron	374
nitrotolulene	225
picoline	375
piperidene	356,376
proline	356
pyridine	356,376
simazine	362
theophylline	356
thymine	377
trietazine	362

the basis of the experimentally determined adsorption constants and eq 41. The predicted rates were much lower than the actual photodegradation rates at low $C_{\text{Red,eq}}$ and higher than the observed photodegradation rates at high $C_{\text{Red,eq}}$. A rapid release of photogenerated $\cdot\text{OH}$ radicals from the surface or the photoadsorption of substrates may account for these differences.

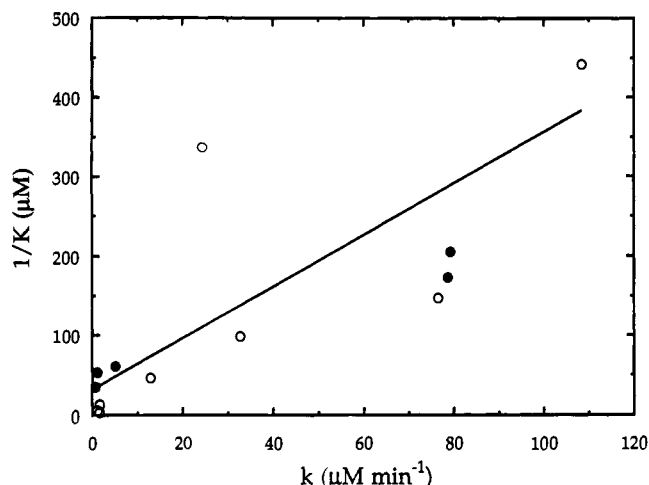
The apparent adsorption constants, K , and the apparent photodegradation rate constants, k , vary over a wide range and appear to be dependent upon the exact experimental conditions for the photocatalytic oxidation of phenol and 4-chlorophenol on TiO_2 (Degussa P25). The sorption constant, K , is expected to remain relatively constant over various conditions if it truly reflects the adsorption affinity of a substrate for a surface. The apparent variability of K indicates the inadequacy of the traditional interpretation of K as an intrinsic adsorption (thermodynamic) constant. Turchi and Ollis⁶⁷ have shown that four different reaction schemes yield the same general rate equation of the basic Langmuir-Hinshelwood form (eq 41) with two independent parameters k and K . According to their kinetic models, the fundamental interpretation of K is different for each reaction scheme, while k is a function only of catalyst properties and light intensities irrespective of which of the four cases is considered. However, K and k , which are supposed to be two independent parameters, seem to be dependent on each other as shown in Figure 11. One possible explanation for this behavior is that various equilibrium adsorption constants involved are changed under the photostationary conditions (e.g., photoadsorption and photodesorption). In these cases, K appears to be a function of light intensity and is dependent on k .

Table 4. Semiconductor Photodegradation of Hydrocarbons, Carboxylic Acids, Alcohols, Halocarbons, and Heteroatom Compounds

substrate	refs
1,3-butadiene	378
1,2-dibromoethane	379
2,2,5-trimethylpentane	225
2-ethoxyethanol	380
2-methoxyethanol	225
acenaphthene	381
acetone	217,225,254,311
benzene	66,225,326,382,383
ethylbenzene	110
benzoic acid	73,76,77,210,309,311,312, 326,339,384,385
bromoform	325
catechol	64,304,386
cresols	97,113,387
cyclohexane	388
diethyl phthalate	360
di- <i>n</i> -butyl phthalate	389
ethylene	378,390
formaldehyde	217
hexane	183
2-propanol	75,83,226,230,243,272, 311,391-396
malathion	305
methanol	75,86,210,225,288,309,311, 397-399
methyl vinyl ketone	108
naphthalene	312
phenol	64,74,76,82,91,98,99,139,195, 204,239,242,251,284,318, 383,400-411
polynuclear aromatics	412
propene	378,413,414
<i>tert</i> -butyl alcohol	75,415
toluene	98,225,321,337,382,416
xylene	217
1,3-diphenylisobenzofuran	417
bromodecane	418
bromododecane	418
dodecanol	418
1-propanol	311,398,419
fluorophenols	304
(4-thiophenyl)-1-butanol	420
4-hydroxybenzyl alcohol	83
acetic acid	51,52,84,210,227,235,309, 311,421-426
acetophenone	382,394
adipic acid	385
alkylphenols	427
1-butanol	217,398,428
butadiene	378
butyric acid	422,429
cyclohexene	388,430
cyclohexanedicarboxylic acid	431
dibromomethane	379
diphenyl sulfide	432
dodecane	418
dodecyl sulfate	418,433
dodecylbenzene sulfonate	55,434
ethane	435,436
ethanol	75,210,301,309,311,326,396, 398,419,432,433,437,438
ethyl acetate	311
formic acid	147,185,210,251,254,309,311, 326,434-436
isobutane	297-299
isobutene	297,298,300,378,413
lactic acid	231
oxalic acid	254,429,439
propionic acid	51,254,422
pyridine	356,376,440
salicylic acid	76,210,251,301,309,311, 326,369,441
sucrose	210,311
tetrafluoroethylene	390

Table 5. Langmuir–Hinshelwood Rate Constants (k) and Adsorption Constants (K) for Photocatalytic Systems Utilizing TiO₂ (Degussa-P25) for Phenol and 4-Chlorophenol (4-CP) Degradation

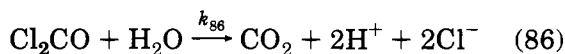
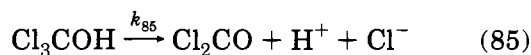
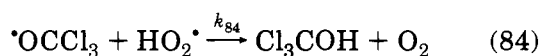
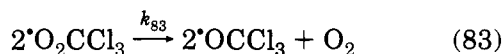
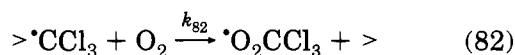
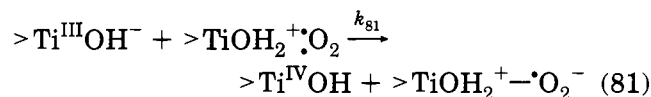
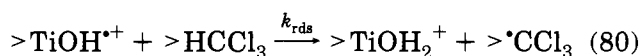
substrate	k ($\mu\text{M min}^{-1}$)	K (μM^{-1})	experimental conditions	ref
phenol	24.4	2.97×10^{-3}	[TiO ₂] = 2 g L ⁻¹ , 125 W Hg lamp, pH 6	405
phenol	12.9	2.19×10^{-2}	[TiO ₂] = 1 g L ⁻¹ , 15 W blacklight (350 nm)	441
phenol	32.7	1.02×10^{-2}	[TiO ₂] = 1 g L ⁻¹ , 15 W germicidal lamp (254 nm)	441
phenol	1.67	3.00×10^{-1}	[TiO ₂] = 1 g L ⁻¹ , 100 W Hg lamp, pH 5.5	74
phenol	1.15	1.80×10^{-1}	[TiO ₂] = 1 g L ⁻¹ , 100 W Hg lamp, pH 3.5	74
phenol	1.70	7.68×10^{-2}	[TiO ₂] = 1 g L ⁻¹ , 100 W Hg lamp, pH 8.5	74
phenol	76.5	6.78×10^{-3}	[TiO ₂] = 1 g L ⁻¹ , 20 W blacklight, pH 3.5	309
phenol	108.4	2.26×10^{-3}	immobilized TiO ₂ film, 20 W blacklight, pH 3.6	311
4-CP	78.6	5.78×10^{-3}	[TiO ₂] = 1 g L ⁻¹ , 20 W blacklight, pH 3.5	309
4-CP	0.77	2.90×10^{-2}	[TiO ₂] = 0.5 g L ⁻¹ , 48 W blacklight, pH 2	107
4-CP	5.17	1.66×10^{-2}	[TiO ₂] = 2 g L ⁻¹ , 125 W Hg lamp ($\lambda > 340$ nm)	112
4-CP	1.2	1.90×10^{-2}	immobilized TiO ₂ film, 90 W blacklight, pH 5.8	306
4-CP	79.3	4.88×10^{-3}	immobilized TiO ₂ film, 20W blacklight, pH 3.6	311

**Figure 11.** Plot of $1/K$ vs k from Table 5 for phenol (○) and 4-chlorophenol (●).

IX. Mechanistic Aspects of Selected Reactions

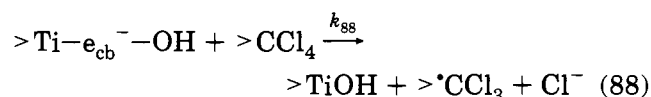
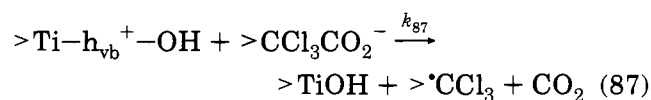
A. Chloroform

Kormann et al.⁵⁰ have proposed the following mechanism for chloroform oxidation after generation of the electron–hole pair due to excitation at wavelengths less than 380 nm:



We believe that similar mechanisms are operative for a wide range of oxidizable chlorinated hydrocarbons

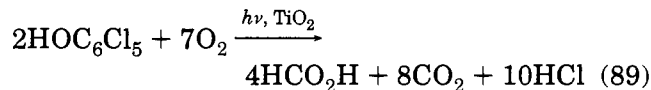
with abstractable hydrogen atoms. In the case of chlorinated hydrocarbons with no abstractable hydrogen atoms or with tetravalent carbon in C(IV) state, reactions can be initiated by direct hole or electron transfer as in the case of trichloroacetic acid or carbon tetrachloride, respectively:



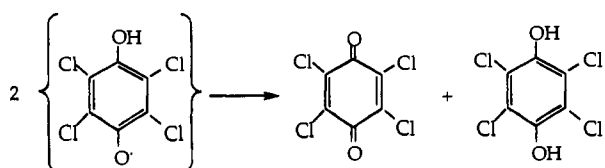
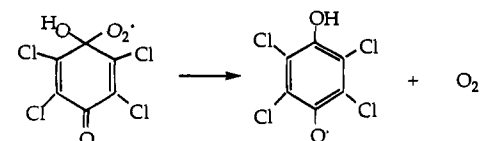
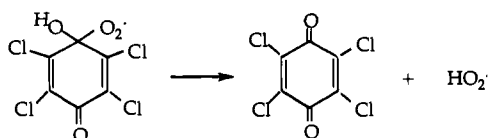
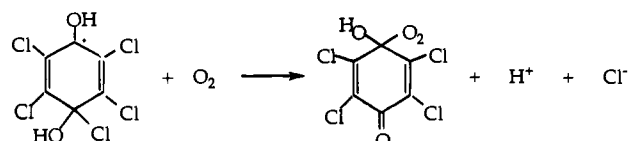
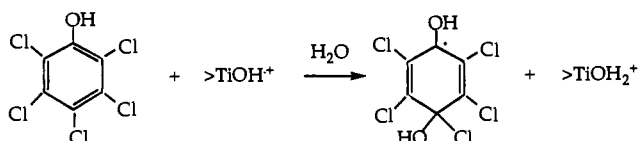
We note that the identical carbon-centered $\text{CCl}_3\cdot$ radical is generated either by direct hole transfer (i.e., the photo-Kolbe process of eq 87) or by direct electron transfer to the carbon(IV) center. The $\text{CCl}_3\cdot$ radical then continues to react via eqs 82–86.

B. Pentachlorophenol

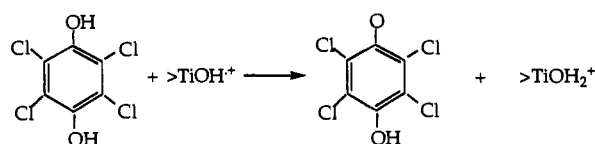
Pentachlorophenol ($\text{C}_6\text{Cl}_5\text{OH}$, PCP) has been used widely as a pesticide and a wood preservative. The photooxidation of PCP in the presence of TiO₂ proceeds via the following stoichiometry:



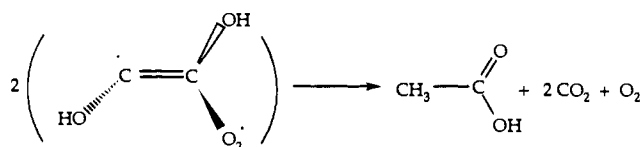
In homogeneous solution, photolysis of PCP has been shown to produce toxic byproducts such as tetrachlorodioxins; however, in the presence of illuminated TiO₂ suspensions, the intermediate dioxins are effectively destroyed.⁴⁹ Mills et al.⁴⁹ reported that complete dechlorination of 47 μM PCP was achieved after 3 h of illumination at high intensity with apparent quantum efficiencies for (Φ_{PCP} , Φ_{Cl^-} , Φ_{H^+} , $\Phi_{\text{H}_2\text{O}_2}$) ranging from 1 to 3%. *p*-Chloranil, tetrachlorohydroquinone, H_2O_2 , and *o*-chloranil were formed as the principal intermediates. Formate and acetate were formed as products during the latter stages of photooxidation. The mechanism for photooxidation of PCP appears to proceed primarily via hydroxyl radical attack on the para position of the PCP ring to form a semiquinone radical which in turn disproportionates to yield *p*-chloranil and tetrachlorohydroquinone. The initial steps in the photocatalytic degradation of PCP as proposed by Mills et al. are as follows:



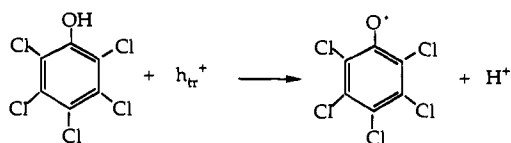
Under high-intensity illumination, the PCP-OH reaction intermediates are attacked further by $\cdot\text{OH}$ to yield HCO_2^- , CH_3CO_2^- , CO_2 , H^+ , and Cl^- with initiation as follows:



Ring fragmentation appears to be a slow process and probably occurs between carbon atoms of the ring which have no chlorine atoms, since chloroacetic acid is not found among the detectable products. The formation of acetate appears to involve a reduction of carbon centers and probably proceeds via disproportionation reactions of free-radical intermediates as proposed below for a likely ring-fragmentation biradical:

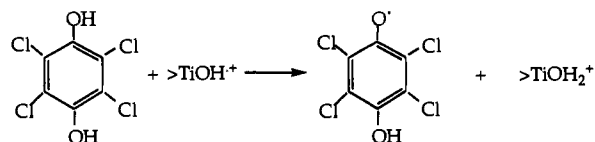


The direct electron-transfer reaction between a surface-trapped hole and a surface-bound PCP molecule is expected to yield a phenoxy radical as follows:



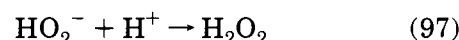
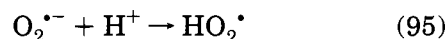
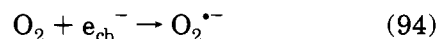
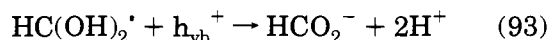
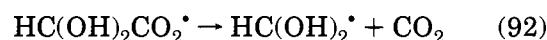
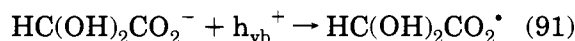
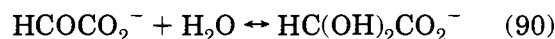
The resulting pentachlorophenoxy radical is most probably a strong oxidant which will be reduced by electrons from the conduction band or by peroxide radicals to regenerate PCP, thus yielding a closed-loop reaction with no net degradation (vide infra).

Experimental results⁴⁹ suggest that $\cdot\text{OH}$ radicals react at least 10 times faster with tetrachlorohydroquinone than with *p*-chloranil:

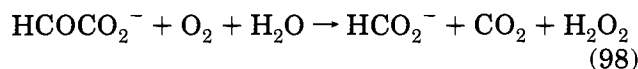


C. Glyoxylic Acid

Carraway et al.⁵¹ have reported that glyoxylate (HCOCO_2^-) is rapidly oxidized to formate on the surface of illuminated Q-sized ZnO colloids over a broad range of pH. The intermediate product, formate, in turn serves as an effective electron donor with the concomitant reduction of dioxygen. On the basis of their kinetic studies Carraway et al. have proposed the following mechanism to account for their kinetic observations:



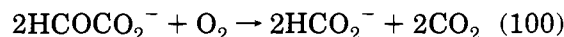
The net reaction occurring on ZnO, obtained by summing the oxidative and reductive steps, is as follows:



In addition, glyoxylate is known to react homogeneously with hydrogen peroxide as follows:

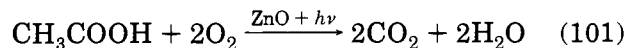


This dark reaction couples to eq 98 to yield the following overall photocatalyzed reaction:



D. Acetic Acid

Carraway et al.⁵¹ have also studied the photocatalytic oxidation of acetate (CH_3CO_2^-) on Q-sized ZnO colloids in which the overall stoichiometry is as follows:

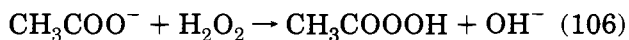
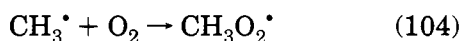
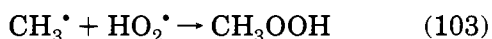
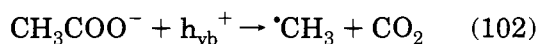


The reaction intermediates were determined to be

HCO_2^- , CHOCO_2^- , HCHO , CH_3OOH , CH_3COOOH , and H_2O_2 . Formate and glyoxylate also serve as effective electron donors on illuminated ZnO surfaces. The relative reactivity of electron donors toward photooxidation was found to occur in the following order: $\text{CHOCO}_2^- > \text{HCO}_2^- > \text{HCHO} > \text{CH}_3\text{CO}_2^- > \text{H}_2\text{O}_2 > \text{CH}_3\text{COOOH} > \text{CH}_3\text{OOH}$. The product distributions were analyzed in terms of pathways involving direct oxidation of surface-bound acetate by valence-band holes (or trapped holes) and the indirect oxidation of acetate by surface-bound hydroxyl radicals. The product distribution observed at low photon fluxes indicates that both pathways occur in parallel.

Carraway et al.⁵¹ have proposed a reaction mechanism involving the reaction of an intermediate carbon-centered radical with $>\text{ZnOH}$ surface sites. When electron donors are strongly adsorbed to semiconductor surfaces, surface-mediated reactions appear to play a dominant role in determination of the time-dependent product distributions.

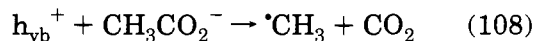
The formation of methyl hydroperoxide and peroxyacetic acid as reaction intermediates during the course of acetate oxidation appears to be consistent with the following mechanism:



Wolff et al.²⁹⁷ have examined the photocatalytic oxidation of acetate on TiO_2 in an attempt to answer the question of the intermediacy of $\cdot\text{OH}$ radicals in photocatalytic systems. It has been established in detailed radiation chemical investigations that hydroxyl radicals attack acetate ions mainly at the methyl group:²⁹⁸



In the presence of oxygen, the radicals thus formed react quickly with molecular oxygen leading to the formation of CHOCO_2H , HOCH_2COOH , $\text{HO}_2\text{CH}_2\text{OCH}_2\text{CO}_2\text{H}$, HCHO , and CO_2 . Direct electrochemical oxidation of acetate results in the well-known Kolbe decarboxylation with the formation of a methyl radical:

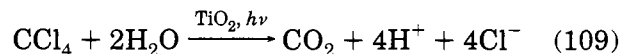


In this case, the product distribution should include CH_3COOH , CH_3OCH_3 , HCHO , CH_3OH , HCOOH , and H_2O_2 . Wolff et al.²⁹⁷ reported that at pH 10.6, the main products of the photocatalytic oxidation of acetate on TiO_2 were glycolate and formate. Glyoxylate was also detected at relatively short illumination times. On the other hand, under acidic conditions they found only formate and formaldehyde. As noted by Carraway et al.⁵¹ glycolate and glyoxylate are readily oxidized in the presence of TiO_2 under band-gap illumination. They argue that these observations are consistent with reactions initiated by hydroxyl

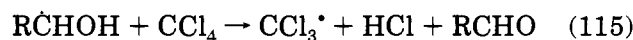
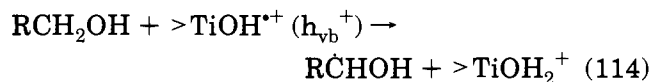
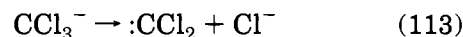
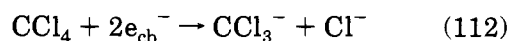
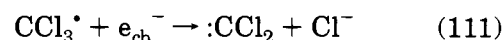
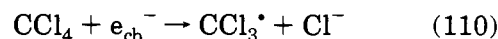
radicals, since decarboxylation of glycolate should only result in C_1 products such as methanol or formate. The formation of glycolate and glyoxylate is thus taken as evidence for the oxidation of acetate via hydroxyl radicals. The relative importance of the hydroxyl radical pathway appears to be higher with increasing pH. Since the TiO_2 is negatively charged above pH 6.5 (vide supra) electrostatic repulsion should hinder the inner-sphere adsorption of acetate molecule thus favoring an attack of surface bound hydroxyl radicals on the methyl group. On the other hand, negatively charged carboxylate groups are attracted toward positively charged surface groups of the metal oxide semiconductor particles at pH values below the pH_{zpc} ; this attraction leads to an inner-sphere coordination through $>\text{TiOH}$ groups. When an electron donor is strongly bound via inner-sphere sorption at the surface, electron transfer appears to occur via the valence-band holes or trapped holes on the surface. This pathway clearly favors direct decarboxylation of the acetate.

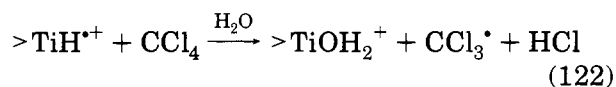
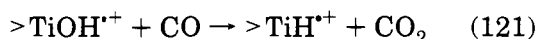
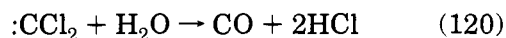
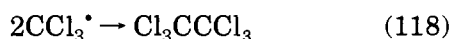
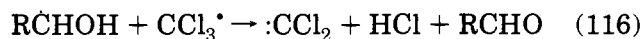
E. Carbon Tetrachloride

Choi and Hoffmann²⁹⁹ have investigated the photo-reductive degradation of carbon tetrachloride (CCl_4) on TiO_2 in aqueous suspensions in the presence of a variety of organic electron donors (alcohols, carboxylic acids, and benzene derivatives) over a broad range of pH. CHCl_3 , C_2Cl_4 , and C_2Cl_6 were detected as intermediates during photolysis:

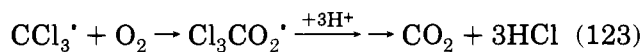


The rate of CCl_4 dechlorination can be enhanced significantly when alcohols and organic acids are used as electron donors. Kinetic isotope effects and structure-reactivity relationships show that hydrogen abstraction by hydroxyl radicals plays an important role in hole-scavenging mechanisms. Choi and Hoffmann²⁹⁹ argue that the pH of the TiO_2 suspension influences the rate of CCl_4 reduction either by altering the electrostatic interactions of electron donors on the TiO_2 surface or by changing the reduction potential of the conduction band electron in a Nernstian fashion. They also report that dissolved oxygen is nonessential for complete mineralization of CCl_4 . To account for these results Choi and Hoffmann²⁹⁹ propose a reaction mechanism in the absence of oxygen, which involves dichlorocarbene formation through a two-electron transfer pathway initiated by conduction-band electron transfer as follows:





In the presence of oxygen, the following additional steps appear to be operative:



Hilgendorff et al.³⁰⁰ have also studied the degradation of CCl_4 in detail. They report the rate of CCl_4 degradation is not enhanced by the presence of Pt islands which are often known to reduce the overpotential of heterogeneous electron-transfer processes (e.g., for the reduction of protons to molecular hydrogen). The absence of a catalytic effect of the platinum deposits could either be explained by a small overpotential for the reaction or by a failure of Pt islands on the TiO_2 surface to transfer electrons to CCl_4 rather than to H_2O or protons.

The pH-independent polarographic reduction potential $E_{1/2}$ of CCl_4 is -0.51 V while the conduction-band reduction potential of TiO_2 is known to follow standard Nernstian behavior as follows:

$$E_{\text{Red}} = (-0.1 \text{ to } 0.059 \text{ pH}) \text{ V} = -0.572 \text{ V at pH } 8 \quad (124)$$

Thus the reduction potential of the conduction band electrons above pH 8 should be sufficient to reduce carbon tetrachloride according to eqs 110–112 above.

Hilgendorff et al.³⁰⁰ report that the rate of degradation of CCl_4 is enhanced considerably in the presence of a hole scavenger such as 2-methyl-2-propanol due to the formation of the 2-methyl-2-propanol radical. This β -hydroxyl radical is not capable of direct CCl_4 reduction (as are the α -hydroxy radicals) nor is it able to inject an electron in the conduction band of TiO_2 to yield a current-doubling effect. Hilgendorff et al. propose that 2-methyl-2-propanol inhibits the electron-hole recombination by increasing the number of electrons in the semiconductor particle which can induce the reduction of CCl_4 via reaction. On the other hand, the α -hydroxy radicals formed according to the above mechanism during the one-electron (hole) oxidation of 2-propanol, ethanol, and methanol are able to reduce CCl_4 as well as to inject an electron into the TiO_2 -conduction band. Hilgendorff et al.³⁰⁰ report that the quantum yield of CCl_4 degradation increases by a factor of 80 in oxygen-free solutions due to the absence of competition from O_2 for conduction-band electrons and to the lack of scavenging of the α -hydroxy radicals by O_2 .

F. 4-Chlorophenol

The formation of several different surface structures by an adsorbate may be expected to yield several concurrent reaction pathways. Mills et al.^{8,107} determined that the photooxidation of 4-chlorophenol ($\text{ClC}_6\text{H}_4\text{OH}$) is best described by three concurrent reaction pathways. One reaction pathway leads to an unstable intermediate that undergoes ring cleavage and subsequent rapid decarboxylation and dechlorination. The other two reaction pathways result in stable intermediates, including hydroquinone (HQ) and 4-chlorocatechol (4-CC). The addition of inorganic oxidants such as ClO_2^- , $\text{S}_2\text{O}_8^{2-}$, ClO_3^- , IO_4^- , and BrO_3^- increases the rate of degradation of 4-CP.^{301,303} Consistent with Mills' explanation and other previous mechanistic studies,^{23,54,301,304–306} the reactions shown in Figure 12 explain the effects of ClO_3^- and the formation of intermediates.²⁹⁶

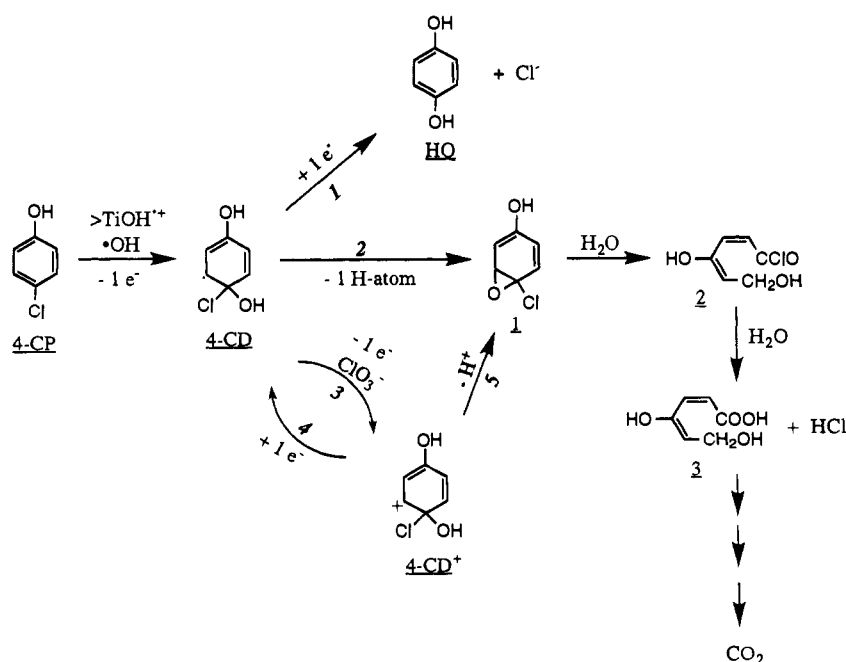


Figure 12. Reaction scheme for the degradation of 4-CP in the presence of ClO_3^- .

According to the mechanism shown in Figure 12, three parallel reaction pathways are open; these pathways proceed in parallel after the initial hydroxylation of 4-CP to form the 4-chlorodihydroxycyclodiethyl radical (4-CD). Reduction by a conduction-band electron (pathway 1) yields HQ and Cl^- . Abstraction of an H-atom (2) occurs by an active oxygen species (e.g., HO_2^* or HO^*) or by the two-step process of electron abstraction by a valence-band hole followed by deprotonation. The resultant unstable intermediate, 1, is hydrolyzed to form a ring-opened acid chloride, 2, which itself hydrolyzes to a carboxylic acid, 3, and releases HCl. Abstraction of an electron (3) from 4-CD to yield 4-CD^+ is facilitated by ClO_3^- . Subsequently, 4-CD^+ either undergoes a back-reaction to 4-CD (4) via reduction by a conduction-band electron or deprotonates (5) to form 1 and subsequent products, 2 and 3.

The pathways are not equally efficient with respect to photooxidation. Pathway 2 proceeds through three thermal oxidation steps subsequent to its initiation by one photon. Pathway 3, on the other hand, provides no additional fast thermal oxidation steps and 4-CD^+ exhausts additional photogenerated charge carriers via the reductive pathway 4 by undergoing further oxidation with valence-band holes and hydroxyl radicals. In general, the highest oxidation quantum efficiencies are expected by the selection of pathways such as 2 for which a maximum number of thermal oxidation steps occur. The ClO_3^- anion is a selecting agent for pathway 3. Whereas reducing the rate of charge-carrier recombination and increasing the rate of the primary interfacial charge transfer are well-known strategies to increase catalyst performance, the implication for heterogeneous photochemistry is that pathway-selecting agents may provide another effective route to higher quantum efficiencies. In addition, macroscopic measurements of quantum efficiencies based upon product yields may not be representative of the branching ratio between charge-carrier recombination and interfacial charge transfer due to thermal oxidative events initiated by a photooxidative event.

X. Conclusions

Semiconductor photocatalysis appears to be a promising technology that has a number of applications in environmental systems such as air purification, water disinfection, hazardous waste remediation, and water purification. In addition, the basic research that underlies the application of this technology is forging a new understanding of the complex heterogeneous photochemistry of metal oxide systems in multiphase environments.

XI. Acknowledgments

We are grateful to ARPA (Advanced Research Projects Agency), ONR (Office of Naval Research) [NAV 5 HFMN N0001492J1901] and the Alexander von Humboldt Foundation for financial support. S. Martin is supported by a National Defense Science and Engineering Graduate Fellowship.

XII. References

- Rife, R.; Thomas, T. W.; Norberg, D. W.; Fournier, R. L.; Rinker, F. G.; Bonomo, M. S. *Environ. Prog.* **1989**, *8*, 167–173.
- Pojasek, R. B. *Toxic and Hazardous Waste Disposal*; Ann Arbor Science: Ann Arbor, MI, 1979; Vols. I–IV.
- Kim, B. J.; Gee, C. S.; Bandy, J. T.; Huang, C. S. *J. Water Pollut. Control Fed.* **1991**, *63*, 501–509.
- Freeman, H. M. *Incinerating Hazardous Wastes*; Technomic Publishing Co.: Lancaster, PA, 1988; p 375.
- De Renzo, D. J. *Biodegradation Techniques for Industrial Organic Wastes*; Noyes Data Corporation: Park Ridge, NJ, 1980; p 358.
- Photocatalytic Purification and Treatment of Water and Air*; Ollis, D. F., Al-Ekabi, H., Ed.; Elsevier: Amsterdam, 1993.
- Blake, D. M. *Bibliography of Work on the Photocatalytic Removal of Hazardous Compounds from Water and Air*. National Renewal Energy Laboratory, 1994.
- Mills, A.; Davies, R. H.; Worsley, D. *Chem. Soc. Rev.* **1993**, *22*, 417–425.
- Kamat, P. V. *Chem. Rev.* **1993**, *93*, 267–300.
- Fox, M. A.; Dulay, M. T. *Chem. Rev.* **1993**, *93*, 341–357.
- Bahnemann, D. W. *Isr. J. Chem.* **1993**, *33*, 115–136.
- Pichat, P. *Catal. Today* **1994**, *19*, 313–333.
- Aithal, U. S.; Aminabhavi, T. M.; Shukla, S. S. *J. Hazard. Mater.* **1993**, *33*, 369–400.
- Lewis, L. N. *Chem. Rev.* **1993**, *93*, 2693.
- Bahnemann, D.; Cunningham, J.; Fox, M. A.; Pelizzetti, E.; Serpone, N. In *Aquatic and Surface Photochemistry*; Helz, G. R., Zepp, R. G., Crosby, D. G., Eds.; Lewis Publishers: Boca Raton, FL, 1994; pp 261–316.
- Fox, M. A. *Photochem. Photobiol.* **1990**, *52*, 617.
- Ollis, D. F.; Pelizzetti, E.; Serpone, N. *Environ. Sci. Technol.* **1991**, *25*, 1523–1529.
- Pelizzetti, E., Serpone, N., Eds. *Homogeneous and Heterogeneous Photocatalysis*; D. Reidel Publishing Company: Dordrecht, 1986.
- Grätzel, M. *Heterogeneous Photochemical Electron Transfer*; CRC Press: Boca Raton, FL, 1989.
- Matthews, R. W. *Pure Appl. Chem.* **1992**, *64*, 1285–1290.
- Schiavello, M., Ed. *Photocatalysis and Environment: Trends and Applications*; Kluwer Academic Publishers: Dordrecht, 1988.
- Schiavello, M., Ed. *Photoelectrochemistry, Photocatalysis and Photoreactors*; D. Reidel Publishing Company: Dordrecht, 1985.
- Serpone, N.; Lawless, D.; Terzian, R.; Meisel, D. In *Electrochemistry in Colloids and Dispersions*; Mackay, R. A., Texter, J., Eds.; VCH Publishers, Inc.: New York, 1992; pp 399–416.
- Serpone, N., Pelizzetti, E., Eds. *Photocatalysis: Fundamentals and Applications*; John Wiley & Sons: New York, 1989.
- Anpo, M. In *Research on Chemical Intermediates*; Elsevier Science Publishers B.V.: Amsterdam, 1989; p 67.
- Bahnemann, D. W.; Bockelmann, D.; Goslich, R. In *Solar Energy Materials*; Elsevier Science Publishers B.V.: North-Holland, 1991; pp 564–583.
- Henglein, A. *Chem. Rev.* **1989**, *89*, 1861.
- Ireland, J. C.; Klostermann, P.; Rice, E. W.; Clark, R. M. *Appl. Environ. Microbiol.* **1993**, *59*, 1668–1670.
- Sjogren, J. C.; Sierka, R. A. *Appl. Environ. Microbiol.* **1994**, *60*, 344–347.
- Cai, R. X.; Kubota, Y.; Shuin, T.; Sakai, H.; Hashimoto, K.; Fujishima, A. *Cancer Res.* **1992**, *52*, 2346–2348.
- Cai, R.; Hashimoto, K.; Kubota, Y.; Fujishima, A. *Chem. Lett.* **1992**, 427–430.
- Suzuki, K. In *Photocatalytic Purification and Treatment of Water and Air*; Ollis, D. F., Al-Ekabi, H., Eds.; Elsevier: Amsterdam, 1993.
- Karakitsou, K. E.; Verykios, X. E. *J. Phys. Chem.* **1993**, *97*, 1184–1189.
- Grätzel, M. *Acc. Chem. Res.* **1981**, *14*, 376.
- Kalyanasundaram, K.; Borgarello, E.; Duonghong, D.; Grätzel, M. *Angew. Chem., Int. Ed. Engl.* **1981**, *20*, 987.
- Duonghong, D.; Borgarello, E.; Grätzel, M. *J. Am. Chem. Soc.* **1981**, *103*, 4685.
- Borgarello, E.; Kiwi, J.; Pelizzetti, E.; Visca, M.; Grätzel, M. *Nature* **1981**, *289*, 158.
- Wold, A. *Chem. Mater.* **1993**, *5*, 280–283.
- Khan, M.; Rao, N. N. *J. Photochem. Photobiol. A: Chem.* **1991**, *56*, 101–111.
- Schiavello, M. *Electrochim. Acta* **1993**, *38*, 11–14.
- Khan, M.; Chatterjee, D.; Krishnaratnam, M.; Bala, M. *J. Mol. Catal.* **1992**, *72*, 13–18.
- Khan, M.; Chatterjee, D.; Bala, M. *J. Photochem. Photobiol. A: Chem.* **1992**, *67*, 349–352.
- Gerischer, H.; Heller, A. *J. Electrochem. Soc.* **1992**, *139*, 113–118.
- Jackson, N. B.; Wang, C. M.; Luo, Z.; Schwitzgebel, J.; Ekerdt, J. G.; Brock, J. R.; Heller, A. *J. Electrochem. Soc.* **1991**, *138*, 3660–3664.
- Nair, M.; Luo, Z. H.; Heller, A. *Ind. Eng. Chem. Res.* **1993**, *32*, 2318–2323.
- Boer, K. W. *Survey of Semiconductor Physics*; Van Nostrand Reinhold: New York, 1990; p 249.
- Rothenberger, G.; Moser, J.; Grätzel, M.; Serpone, N.; Sharma, D. K. *J. Am. Chem. Soc.* **1985**, *107*, 8054.

- (48) Memming, R. In *Topics in Current Chemistry*; Steckham, E., Ed.; Springer-Verlag: Berlin, 1988; Vol. 143, pp 79–113.
- (49) Mills, G.; Hoffmann, M. R. *Environ. Sci. Technol.* **1993**, *27*, 1681–1689.
- (50) Kormann, C.; Bahnemann, D. W.; Hoffmann, M. R. *Environ. Sci. Technol.* **1991**, *25*, 494–500.
- (51) Carraway, E. R.; Hoffman, A. J.; Hoffmann, M. R. *Environ. Sci. Technol.* **1994**, *28*, 786–793.
- (52) Chemeseddine, A.; Boehm, H. P. *J. Mol. Catal.* **1990**, *60*, 295–311.
- (53) D'Oliveira, J. C.; Minero, C.; Pelizzetti, E.; Pichat, P. *J. Photochem. Photobiol. A: Chem.* **1993**, *72*, 261–267.
- (54) D'Oliveira, J. C.; Al-Sayyed, G.; Pichat, P. *Environ. Sci. Technol.* **1990**, *24*, 990–996.
- (55) Hidaka, H.; Zhao, J.; Pelizzetti, E.; Serpone, N. *J. Phys. Chem.* **1992**, *96*, 2226–2230.
- (56) Pelizzetti, E.; Minero, C.; Piccinini, P.; Vincenti, M. *Coord. Chem. Rev.* **1993**, *125*, 183–193.
- (57) Albert, M.; Gao, Y. M.; Toft, D.; Dwight, K.; Wold, A. *Mater. Res. Bull.* **1992**, *27*, 961–966.
- (58) Inel, Y.; Ertek, D. *J. Chem. Soc., Faraday Trans.* **1993**, *89*, 129–133.
- (59) Borgarello, E.; Serpone, N.; Emo, G.; Harris, R.; Pelizzetti, E.; Minero, C. *Inorg. Chem.* **1986**, *25*, 4499–4503.
- (60) Martin, S. T.; Herrmann, H.; Choi, W.; Hoffmann, M. R. *Trans. Faraday Soc.* **1994**, *90*, 3315–3323.
- (61) Martin, S. T.; Herrmann, H.; Hoffmann, M. R. *Trans. Faraday Soc.* **1994**, *90*, 3323–3330.
- (62) Stumm, W. *Chemistry of the Solid-Water Interface*; Wiley-Interscience: New York, 1992; p 428.
- (63) Bickley, R. I.; Gonzalez-Carreno, T.; Lees, J. S.; Palmisano, L.; Tilley, R. J. D. *J. Solid State Chem.* **1991**, *92*, 178.
- (64) Augugliaro, V.; Palmisano, L.; Sclafani, A.; Minero, C.; Pelizzetti, E. *Toxicol. Environ. Chem.* **1988**, *16*, 89–109.
- (65) Ollis, D. F.; Hsiao, C. Y.; Budiman, L.; Lee, C. L. *J. Catal.* **1984**, *88*, 89–96.
- (66) Turchi, C. S.; Ollis, D. F. *J. Catal.* **1989**, *119*, 480.
- (67) Turchi, C. S.; Ollis, D. F. *J. Catal.* **1990**, *122*, 178.
- (68) Terzian, R.; Serpone, N.; Draper, R. B.; Fox, M. A.; Pelizzetti, E. *Langmuir* **1991**, *7*, 3081–3089.
- (69) Noda, H.; Oikawa, K.; Kamada, H. *Bull. Chem. Soc. Jpn.* **1993**, *66*, 455–458.
- (70) Anpo, M.; Shima, T.; Kubokawa, Y. *Chem. Lett.* **1985**, 1799.
- (71) Jaeger, C. D.; Bard, A. J. *J. Phys. Chem.* **1979**, *83*, 3146.
- (72) Mao, Y.; Schoneich, C.; Asmus, K. D. *J. Phys. Chem.* **1991**, *95*, 80–89.
- (73) Moser, J.; Punchedewa, S.; Infelta, P. P.; Grätzel, M. *Langmuir* **1991**, *7*, 3012.
- (74) Matthews, R. W.; McEvoy, S. R. *J. Photochem. Photobiol. A: Chem.* **1992**, *64*, 231–246.
- (75) Ohtani, B.; Nishimoto, S. *J. Phys. Chem.* **1993**, *97*, 920–926.
- (76) Tunesi, S.; Anderson, M. J. *J. Phys. Chem.* **1991**, *95*, 3399–3405.
- (77) Tunesi, S.; Anderson, M. A. *Langmuir* **1992**, *8*, 487–495.
- (78) Phillips, L. A.; Raupp, G. B. *J. Mol. Catal.* **1992**, *77*, 297–311.
- (79) Stafford, U.; Gray, K. A.; Kamat, P. V.; Varma, A. *Chem. Phys. Lett.* **1993**, *205*, 55–61.
- (80) Richard, C.; Lemaire, J. *J. Photochem. Photobiol. A: Chem.* **1990**, *55*, 127.
- (81) Draper, R. B.; Fox, M. A. *Langmuir* **1990**, *6*, 1396–1402.
- (82) Grabner, G.; Li, G. Z.; Quint, R. M.; Quint, R.; Getoff, N. *J. Chem. Soc., Faraday Trans.* **1991**, *87*, 1097–1101.
- (83) Richard, C. *J. Photochem. Photobiol. A: Chem.* **1993**, *72*, 179–182.
- (84) Kormann, C.; Bahnemann, D. W.; Hoffmann, M. R. *Environ. Sci. Technol.* **1988**, *22*, 798–806.
- (85) Hoffmann, A. J.; Carraway, E. R.; Hoffmann, M. R. *Environ. Sci. Technol.* **1994**, *28*, 776–785.
- (86) Wang, C. M.; Heller, A.; Gerischer, H. *J. Am. Chem. Soc.* **1992**, *114*, 5230–5234.
- (87) Gerischer, H.; Heller, A. *J. Phys. Chem.* **1991**, *95*, 5261–5267.
- (88) Hsiao, C. Y.; Lee, C. L.; Ollis, D. F. *J. Catal.* **1983**, *82*, 418–423.
- (89) Pruden, A. L.; Ollis, D. F. *J. Catal.* **1983**, *82*, 404–417.
- (90) Mills, A.; Morris, S.; Davies, R. *J. Photochem. Photobiol. A: Chem.* **1993**, *70*, 183.
- (91) Okamoto, K.; Yamamoto, Y.; Tanaka, H.; Tanaka, M.; Itaya, A. *Bull. Chem. Soc. Jpn.* **1985**, *58*, 2015–2022.
- (92) Kormann, C.; Bahnemann, D. W.; Hoffmann, M. R. *J. Phys. Chem.* **1988**, *92*, 5196–5201.
- (93) Bahnemann, D. W.; Kormann, C.; Hoffmann, M. R. *J. Phys. Chem.* **1987**, *91*, 3789–3798.
- (94) Faust, B. C.; Hoffmann, M. R.; Bahnemann, D. W. *J. Phys. Chem.* **1989**, *93*, 6371.
- (95) Faughnam, J.; Morgan, J. J.; Hoffmann, M. R. SURFEQL—An Interactive Code for the Calculation of Chemical Equilibria in Aqueous Solution and on Metal Oxide Surfaces. California Institute of Technology, 1981.
- (96) Bravo, A.; Garcia, J.; Domenech, X.; Peral, J. *J. Chem. Res. S* **1993**, 376–377.
- (97) Brezova, V.; Stasko, A. *J. Catal.* **1994**, *147*, 156–162.
- (98) Butler, E. C.; Davis, A. P. *J. Photochem. Photobiol. A: Chem.* **1993**, *70*, 273–283.
- (99) Davis, A. P.; Huang, C. P. *Chemosphere* **1993**, *26*, 1119–1135.
- (100) Jenny, B.; Pichat, P. *Langmuir* **1991**, *7*, 947–954.
- (101) Krosley, K. W.; Collard, D. M.; Adamson, J.; Fox, M. A. *J. Photochem. Photobiol. A: Chem.* **1993**, *69*, 357–360.
- (102) Ku, Y.; Hsieh, C. B. *Water Res.* **1992**, *26*, 1451–1456.
- (103) Lozano, A.; Garcia, J.; Domenech, X.; Casado, J. *J. Photochem. Photobiol. A: Chem.* **1992**, *69*, 237–240.
- (104) Lu, M. C.; Roam, G. D.; Chen, J. N.; Huang, C. P. *J. Photochem. Photobiol. A: Chem.* **1993**, *76*, 103–110.
- (105) Milis, A.; Domenech, X. *J. Photochem. Photobiol. A: Chem.* **1993**, *72*, 55–59.
- (106) Milis, A.; Peral, J.; Domenech, X.; Navio, J. A. *J. Mol. Catal.* **1994**, *87*, 67–74.
- (107) Mills, A.; Morris, S. *J. Photochem. Photobiol. A: Chem.* **1993**, *71*, 75–83.
- (108) Muneer, M.; Das, S.; Manilal, V. B.; Haridas, A. *J. Photochem. Photobiol. A: Chem.* **1992**, *63*, 107–114.
- (109) Trillas, M.; Peral, J.; Domenech, X. *Appl. Catal. B Environ.* **1993**, *3*, 45–53.
- (110) Vidal, A.; Herrero, J.; Romero, M.; Sanchez, B.; Sanchez, M. *J. Photochem. Photobiol. A: Chem.* **1994**, *79*, 213–219.
- (111) Zafra, A.; Garcia, J.; Milis, A.; Domenech, X. *J. Mol. Catal.* **1991**, *70*, 343–349.
- (112) Al-Sayyed, G.; D'Oliveira, J. C.; Pichat, P. *J. Photochem. Photobiol. A: Chem.* **1991**, *58*, 99–114.
- (113) Terzian, R.; Serpone, N.; Minero, C.; Pelizzetti, E. *J. Catal.* **1991**, *128*, 352–365.
- (114) Pelizzetti, E.; Pramuro, E.; Minero, C.; Serpone, N.; Borgarello, E. In *Photocatalysis and Environment*; Schiavello, M., Ed.; NATO ASI Series; Kluwer Academic Publ.: Dordrecht, Netherlands, 1988; p 527.
- (115) Sabate, J.; Anderson, M. A.; Kikkawa, H.; Edwards, M.; Hill, G. G. *J. Catal.* **1991**, *127*, 127.
- (116) Ollis, D. F.; Pelizzetti, E.; Serpone, N. In *Photocatalysis*; Serpone, N., Pelizzetti, E., Eds.; Wiley Interscience: New York, 1989; p 603.
- (117) Matthews, R. W. In *Photochemical Conversion and Storage of Solar Energy*; Pelizzetti, E., Schiavello, M., Eds.; Kluwer Academic Publ.: Dordrecht, Netherlands, 1988; pp 427–449.
- (118) Hong, A. P.; Bahnemann, D. W.; Hoffmann, M. R. *J. Phys. Chem.* **1987**, *91*, 6245.
- (119) Schwarzenbach, R. P.; Gschwend, P. M.; Imboden, D. M. *Environmental Organic Chemistry*; Wiley-Interscience: New York, 1993; p 681.
- (120) Pehkonen, S.; Siefert, R.; Webb, S.; Hoffmann, M. R. *Environ. Sci. Technol.* **1993**, *26*, 2056.
- (121) Rao, M. V.; Rajeshwar, K.; Vernerker, V. R.; Dubow, J. *J. Phys. Chem.* **1980**, *84*, 1987.
- (122) Nishimoto, S.; Ohtani, B.; Kajiwara, H.; Kagiya, T. *J. Chem. Soc., Faraday Trans. 1* **1985**, *81*, 61.
- (123) Martin, S. T.; Morrison, C. L.; Hoffmann, M. R. *J. Phys. Chem.* **1994**, *98*, 13695.
- (124) Mihaylov, B. V.; Hendrix, J. L.; Nelson, J. H. *J. Photochem. Photobiol. A: Chem.* **1993**, *72*, 173–177.
- (125) Domenech, X. In *Photocatalytic Purification and Treatment of Water and Air*; Ollis, D. F., Al-Ekabi, H., Eds.; Elsevier: Amsterdam, 1993; pp 337–351.
- (126) Peral, J.; Domenech, X. *J. Chem. Technol. Biotechnol.* **1992**, *53*, 93–96.
- (127) Peral, J.; Munoz, J.; Domenech, J. *Photochem. Photobiol.* **1990**, *55*, 251.
- (128) Tanaka, K.; Hisanaga, T.; Rivera, A. P. In *Photocatalytic Purification and Treatment of Water and Air*; Al-Ekabi, H., Ollis, D. F., Eds.; Elsevier: Amsterdam, 1993; pp 169–178.
- (129) Vrachnou, E.; Grätzel, M.; McVoy, A. *J. Electroanal. Chem.* **1989**, *258*, 193.
- (130) Bahnemann, D. W.; Mönig, J.; Chapmann, R. *J. Phys. Chem.* **1987**, *91*, 3782–3788.
- (131) Disdier, J.; Hermann, J.-M.; Pichat, P. *J. Chem. Soc., Faraday Trans. 1* **1983**, *79*, 651.
- (132) Navio, J. A.; Marchena, F. J.; Roncel, M.; Del la Rosa, M. A. *J. Photochem. Photobiol. A: Chem.* **1991**, *55*, 319.
- (133) Grätzel, M.; Howe, R. F. *J. Phys. Chem.* **1990**, *94*, 2566.
- (134) Moser, J.; Grätzel, M.; Gallay, R. *Helv. Chim. Acta* **1987**, *70*, 1596.
- (135) Soria, J.; Conesa, J. C.; Augugliaro, V.; Palmisano, L.; Schiavello, M.; Sclafani, A. *J. Phys. Chem.* **1991**, *95*, 274.
- (136) Bickley, R. I.; Lees, J. S.; Tilley, R. J. D.; Palmisano, L.; Schiavello, M.; Sclafani, A. *J. Chem. Soc., Faraday Trans.* **1992**, *88*, 377.
- (137) Bickley, R. I.; Palmisano, L.; Schiavello, M.; Sclafani, A. *Stud. Surface Sci. Catal.* **1993**, *75*, 2151–2154.
- (138) Sclafani, A.; Palmisano, L.; Schiavello, M. *Res. Chem. Intermed.* **1992**, *18*, 211.
- (139) Palmisano, L.; Augugliaro, V.; Sclafani, A.; Schiavello, M. *J. Phys. Chem.* **1988**, *92*, 6710–6713.
- (140) Kiwi, J.; Grätzel, M. *J. Phys. Chem.* **1986**, *90*, 637.
- (141) Kiwi, J.; Morrison, C. *J. Phys. Chem.* **1984**, *88*, 6146.

- (142) Luo, Z.; Gao, Q. H. *J. Photochem. Photobiol. A: Chem.* **1992**, *63*, 367.
- (143) Sabate, J.; Anderson, M. A.; Kikkawa, H.; Xu, Q.; Cerveramarch, S.; Hill, C. G. *J. Catal.* **1992**, *134*, 36–46.
- (144) Kikkawa, H.; O'Regan, B.; Anderson, M. A. *J. Electroanal. Chem.* **1991**, *309*, 91.
- (145) Navio, J. A.; Macias, M.; Gonzalez-Catalan, M.; De la Rosa, M. A. *J. Mater. Sci.* **1992**, *27*, 3036.
- (146) Anpo, M.; Kubokawa, Y. *Rev. Chem. Intermed.* **1987**, *8*, 105.
- (147) Aguado, M. A.; Anderson, M. A. *Solar Energy Mater. Solar Cells* **1993**, *28*, 345–61.
- (148) Barbeni, M.; Pelizzetti, E.; Borgarello, E.; Grätzel, M.; Serpone, N. *Int. J. Hydrogen Energy* **1985**, *10*, 249–53.
- (149) Lee, W.; Do, Y. R.; Dwight, K.; Wold, A. *Mater. Res. Bull.* **1993**, *28*, 1127–1134.
- (150) Choi, W.; Termin, A.; Hoffmann, M. R. *J. Phys. Chem.* **1994**, *98*, 13669–13679.
- (151) Borgarello, E.; Kiwi, J.; Grätzel, M.; Pelizzetti, E.; Visca, M. *J. Am. Chem. Soc.* **1982**, *104*, 2996.
- (152) Herrmann, J. M.; Disdier, J.; Pichat, P. *Chem. Phys. Lett.* **1984**, *108*, 618.
- (153) Mu, W.; Herrmann, J. M.; Pichat, P. *Catal. Lett.* **1989**, *3*, 73.
- (154) Bockelmann, D.; Goslich, R.; Bahnemann, D. In *Solar Thermal Energy Utilization*; Becker, M., Funken, K.-H., Schneider, G., Eds.; Springer Verlag GmbH: Heidelberg, 1992; Vol. 6, pp 397–429.
- (155) Brus, L. *Appl. Phys. A* **1991**, *53*, 465.
- (156) Weller, H. *Adv. Mater.* **1993**, *5*, 88.
- (157) Weller, H.; Eychmuller, A.; Vogel, R.; Katsikas, L.; Hasselbarth, A.; Giersig, M. *Isr. J. Chem.* **1993**, *33*, 107.
- (158) Weller, H. *Angew. Chem.* **1993**, *32*, 41.
- (159) Grätzel, M. *Nature* **1991**, *349*, 740.
- (160) Henglein, A. *Top. Curr. Chem.* **1988**, *143*, 113.
- (161) Steigerwald, M. L.; Brus, L. E. *Annu. Rev. Mater. Sci.* **1989**, *19*, 471.
- (162) Steigerwald, M. L.; Alivisatos, A. P.; Gibson, J. M.; Harris, T. D.; Kortan, R.; Muller, A. J.; Thayer, A. M.; Duncan, T. M.; Douglass, D. C.; Brus, L. E. *J. Am. Chem. Soc.* **1988**, *110*, 3046.
- (163) Bawendi, M. G.; Steigerwald, M. L.; Brus, L. E. *Annu. Rev. Phys. Chem.* **1990**, *41*, 477–496.
- (164) Bawendi, M. G.; Wilson, W. L.; Rothberg, L.; Carroll, P. J.; Jedju, T. M.; Steigerwald, M. L.; Brus, L. E. *Phys. Rev. Lett.* **1990**, *65*, 1623.
- (165) Bawendi, M. G.; Carroll, P. J.; Wilson, W. L.; L. E., B. *J. Chem. Phys.* **1992**, *96*, 946.
- (166) Marcus, R. A.; Sutin, N. *Biochim. Biophys. Acta* **1985**, *811*, 265.
- (167) Marcus, R. A. *J. Phys. Chem.* **1990**, *94*, 1050.
- (168) Lewis, N. S. *Annu. Rev. Phys. Chem.* **1991**, *42*, 543.
- (169) Hoffman, A. J.; Mills, G.; Yee, H.; Hoffmann, M. R. *J. Phys. Chem.* **1992**, *96*, 5546.
- (170) Hoffman, A. J.; Yee, H.; Mills, G.; Hoffmann, M. R. *J. Phys. Chem.* **1992**, *96*, 5540.
- (171) Anpo, M.; Shima, T.; Kodama, S.; Kubokawa, Y. *J. Phys. Chem.* **1987**, *91*, 4305.
- (172) Nedeljkovic, J. M.; Nenadovic, M. T.; Micic, O. I.; Nozik, A. J. *J. Phys. Chem.* **1986**, *90*, 12.
- (173) Nosaka, Y.; Ohta, N.; Miyama, H. *J. Phys. Chem.* **1990**, *94*, 3752.
- (174) Giuseppe, P.; Langford, C. H.; Vichova, J.; Vleck, A. *J. Photochem. Photobiol. A: Chem.* **1993**, *75*, 67.
- (175) Lee, W.; Gao, Y.-M.; Dwight, K.; Wold, A. *Mater. Res. Bull.* **1992**, *27*, 685.
- (176) Choi, W. Y.; Termin, A.; Hoffmann, M. R. *Angew. Chem.* **1994**, *106*, 1148–1149.
- (177) Choi, W.; Termin, A.; Hoffmann, M. R. *Angew. Chem., Int. Ed. Engl.* **1994**, *33*, 1091.
- (178) Morrison, S. R. *Electrochemistry at Semiconductor and Oxidized Metal Electrodes*; Plenum Press: New York, 1980.
- (179) Faust, B. C.; Hoffmann, M. R. *Environ. Sci. Technol.* **1986**, *20*, 943–948.
- (180) Mills, A.; Morris, S. *J. Photochem. Photobiol. A: Chem.* **1993**, *71*, 285–289.
- (181) Legrini, O.; Oliveros, E.; Braun, A. M. *Chem. Rev.* **1993**, *93*, 671–698.
- (182) Pichat. In *Photoelectrochemistry, Photocatalysis, and Photoreactors*; Schiavello, M., Ed.; Reidel: Boston, 1985; pp 425–55.
- (183) Witier, P.; Estaque, L.; Roberge, P. C.; Kaliaguine, S. *Can. J. Chem. Eng.* **1977**, *55*, 352–4.
- (184) Augugliaro, V.; Palmisano, L.; Schiavello, M. *AIChE J.* **1991**, *37*, 1096–1100.
- (185) Chester, R. C.; Anderson, M.; Read, H.; Esplugas, S. *J. Photochem. Photobiol. A: Chem.* **1993**, *71*, 291–297.
- (186) Hofstadler, K.; Bauer, R.; Novalic, S.; Heisler, G. *Environ. Sci. Technol.* **1994**, *28*, 670–674.
- (187) Chen, L. C.; Chou, T. C. *Ind. Eng. Chem. Res.* **1993**, *32*, 1520–1527.
- (188) Davis, R. J.; Gainer, J. L.; Oneal, G.; Wu, I. W. *Water Environ. Res.* **1994**, *66*, 50–53.
- (189) Dibble, L. A.; Raupp, G. B. *Environ. Sci. Technol.* **1992**, *26*, 492–495.
- (190) Glaze, W. H.; Kenneke, J. F.; Ferry, J. L. *Environ. Sci. Technol.* **1993**, *27*, 177–184.
- (191) Hidaka, H.; Nakamura, T.; Ishizaka, A.; Tsuchiya, M.; Zhao, J. C. *J. Photochem. Photobiol. A: Chem.* **1992**, *66*, 367–374.
- (192) Klausner, J. F.; Martin, A. R.; Goswami, D. Y.; Schanze, K. S. *J. Solar Energy Eng. Trans. ASME* **1994**, *116*, 19–24.
- (193) Lepore, G. P.; Pant, B. C.; Langford, C. H. *Can. J. Chem.* **1993**, *71*, 2051–2059.
- (194) Pacheco, J. E.; Prairie, M. R.; Yellowhorse, L. *J. Solar Energy Eng. Trans. ASME* **1993**, *115*, 123–129.
- (195) Pelizzetti, E.; Minero, C.; Borgarello, E.; Tinucci, L.; Serpone, N. *Langmuir* **1993**, *9*, 2995–3001.
- (196) Sczechowski, J. G.; Koval, C. A.; Noble, R. D. *J. Photochem. Photobiol. A: Chem.* **1993**, *74*, 273–278.
- (197) Venkatadri, R.; Peters, R. W. *Hazard. Waste Hazard. Mater.* **1993**, *10*, 107–149.
- (198) Wyness, P.; Klausner, J. F.; Goswami, D. Y.; Schanze, K. S. *J. Solar Energy Eng. Trans. ASME* **1994**, *116*, 8–13.
- (199) Yamazaki-Nishida, S.; Nagano, K. J.; Phillips, L. A.; Cerveramarch, S.; Anderson, M. A. *J. Photochem. Photobiol. A: Chem.* **1993**, *70*, 95–99.
- (200) Cooper, G.; Ratcliff, M. A. In U.S. Patent Office: U.S. Patent, 1992.
- (201) Haneda, K. In Japanese Patent Office: Japan Patent, 1992.
- (202) Zeltner, W. A.; Hill, J., C. G.; Anderson, M. A. *CHEMTECH* **1993**, *21*–28.
- (203) Braun, A. M. In *Photochemical Conversion and Storage of Solar Energy*; Pelizzetti, E., Schiavello, M., Eds.; Kluwer: Dordrecht, 1991.
- (204) Augugliaro, V.; Inglese, F.; Palmisano, L.; Schiavello, M. *Chem. Biochem. Eng.* **1992**, *6*, 63–70.
- (205) Bahnemann, D. W.; Bockelmann; Goslich, R.; Hilgendorff, M.; Weichgrebe. In *Photocatalytic Purification and Treatment of Water and Air*; Ollis, D. W., Al-Ekabi, H., Eds.; Elsevier: Amsterdam, 1993; pp 301–319.
- (206) Bockelmann, D. Ph.D. Thesis, Technischen Universität Clausthal, 1993.
- (207) Serpone, N.; Borgarello, E.; Harris, R.; Cahill, P.; Borgarello, M.; Pelizzetti, E. *Solar Energy* **1986**, *14*, 121–127.
- (208) Bahnemann, D. W.; Bockelmann, D.; Goslich, R. In *Elektrochem. Energy Umwelttech* **1991**, *124*, 261–281.
- (209) Matthews, R. W. In Australian Patent, 1990.
- (210) Matthews, R. W.; Abdullah, M.; Low, G. K.-C. *Anal. Chim. Acta* **1990**, *233*, 171–179.
- (211) Matthews, R. W. *Solar Energy* **1987**, *38*, 405–413.
- (212) Al-Ekabi, H.; Safarzadeh-Amiri, A.; Story, J.; Sifton, W. Advanced Technology for Destruction of Organic Pollutants by Photocatalysis. Nutech, Ltd., 1990.
- (213) Robertson, M. K.; Henderson, R. B. In U.S. Patent, 1990.
- (214) Sabate, J.; Anderson, M. A.; Aguado, M. A.; Gimenez, J.; Cerveramarch, S.; Hill, C. G. *J. Mol. Catal.* **1992**, *71*, 57–68.
- (215) Anderson, M. A.; Tunesi, S.; Xu, Q. In U.S. Patent Office: U.S. Patent, 1991.
- (216) Anderson, M. A.; Zeltner, W. A. In U.S. Patent Office: U.S. Patent, 1992.
- (217) Peral, J.; Ollis, D. F. *J. Catal.* **1992**, *136*, 554–565.
- (218) Nimlos, M. R.; Jacoby, W. A.; Blake, D. M.; Milne, T. A. *Environ. Sci. Tech.* **1993**, *27*, 732–740.
- (219) Ollis, D. F. In *Photocatalytic Purification and Treatment of Water and Air*; Ollis, D. F., Al-Ekabi, H., Eds.; Elsevier: Amsterdam, 1993; pp 481–494.
- (220) Ibusuki, T.; Takeuchi, K. *J. Mol. Catal.* **1994**, *88*, 93–102.
- (221) Holden, W.; Marcellino, A.; Valic, D.; Weedon, A. C. In *Photocatalytic Purification and Treatment of Water and Air*; Ollis, D. F., Al-Ekabi, H., Eds.; Elsevier: Amsterdam, 1993; pp 393–404.
- (222) T-Raissi, A.; Muradov, N. Z. In *Photocatalytic Purification and Treatment of Water and Air*; Ollis, D. F., Al-Ekabi, H., Eds.; Elsevier: Amsterdam, 1993; pp 435–454.
- (223) Larson, S. A.; Falconer, J. L. In *Photocatalytic Purification and Treatment of Water and Air*; Ollis, D. F., Al-Ekabi, H., Eds.; Elsevier: Amsterdam, 1993; pp 473–479.
- (224) Kutsuna, S.; Takeuchi, K.; Ibusuki, T. *J. Atmos. Chem.* **1992**, *14*, 1–10.
- (225) Lichtin, N. N.; Dong, J.; Vijayakumar, K. M. *Water Pollut. Res. J. Can.* **1992**, *27*, 203–210.
- (226) Kobayakawa, K.; Nakazawa, Y.; Ikeda, M.; Sato, Y.; Fujishima, A. *Ber. Bunsen-Ges. Phys. Chem.* **1990**, *94*, 1439–1443.
- (227) Yoneyama, H. *Res. Chem. Intermed.* **1991**, *15*, 101–111.
- (228) Dagan, G.; Tomkiewicz, M. *J. Phys. Chem.* **1993**, *97*, 12652–12655.
- (229) Aguado, M. A.; Anderson, M. A.; Hill, C. G. *J. Mol. Catal.* **1994**, *89*, 165–178.
- (230) Cunningham, J.; Sedlak, P. *J. Photochem. Photobiol. A: Chem.* **1994**, *77*, 255–263.
- (231) Inoue, H.; Yamachika, M.; Yoneyama, H. *J. Chem. Soc., Faraday Trans.* **1992**, *88*, 2215–2219.
- (232) Mao, Y.; Schoneich, C.; Asmus, K. D. *J. Phys. Chem.* **1992**, *96*, 8522–8529.
- (233) Shiragami, T.; Fukami, S.; Wada, Y. J.; Yanagida, S. *J. Phys. Chem.* **1993**, *97*, 12882–12887.

- (234) Lai, C. W.; Kim, Y. I.; Wang, C. M.; Mallouk, T. E. *J. Org. Chem.* **1993**, *58*, 1393–1399.
- (235) Bideau, M.; Claudel, B.; Faure, L.; Kazouan, H. *J. Photochem. Photobiol. A: Chem.* **1991**, *61*, 269–280.
- (236) Augugliaro, V.; Lopezmunoz, M. J.; Palmisano, L.; Soria, J. *Appl. Catal. A: Gen.* **1993**, *101*, 7–13.
- (237) D'Oliveira, J. C.; Guillard, C.; Maillard, C.; Pichat, P. *J. Environ. Sci. Health Part A: Environ. Sci. Eng.* **1993**, *28*, 941–962.
- (238) Papp, J.; Soled, S.; Dwight, K.; Wold, A. *Chem. Mater.* **1994**, *6*, 496–500.
- (239) Wei, T. Y.; Wan, C. C. *Ind. Eng. Chem. Res.* **1991**, *30*, 1293–1300.
- (240) Pelizzetti, E.; Minero, C.; Carlin, V.; Vincenti, M.; Pramauro, E.; Dolci, M. *Chemosphere* **1992**, *24*, 891–910.
- (241) Inoue, T.; Watanabe, T.; Fujishima, A.; Honda, K. *Chem. Lett.* **1977**, 1073.
- (242) Okamoto, K.; Yamamoto, Y.; Tanaka, H.; Tanaka, M. *Bull. Chem. Soc. Jpn.* **1985**, *58*, 2023–2028.
- (243) Egerton, T. A.; King, C. J. *J. Oil Colour Chem. Assoc.* **1979**, *62*, 386–389.
- (244) Harvey, P.; Rudham, R. *J. Chem. Soc., Faraday Trans. 1* **1988**, *84*, 4181.
- (245) Albery, W. J.; Brown, G. T.; Darwent, J. R.; Saievar-Iranizad, E. *J. Chem. Soc., Faraday Trans. 1* **1985**, *81*, 1999–2007.
- (246) Pollema, C. H.; Milosavljevic, E. B.; Hendrix, J. L.; Solujic, L.; Nelson, J. H. *Monatsh. Chem.* **1992**, *123*, 333–339.
- (247) Cant, N. W.; Cole, J. R. *J. Catal.* **1992**, *134*, 317–330.
- (248) Maldotti, A.; Amadelli, R.; Carassiti, V. *Can. J. Chem.* **1988**, *66*, 76.
- (249) Gonzalez, M.; Chaparro, A. M.; Salvador, P. *J. Photochem. Photobiol. A: Chem.* **1993**, *73*, 221–231.
- (250) Aguado, M. A.; Gimenez, J.; Cerveramarch, S. *Chem. Eng. Commun.* **1991**, *104*, 71–85.
- (251) Prairie, M. R.; Evans, L. R.; Stange, B. M.; Martinez, S. L. *Environ. Sci. Technol.* **1993**, *27*, 1776–1782.
- (252) Bideau, M.; Claudel, B.; Faure, L.; Kazouan, H. *J. Photochem. Photobiol. A: Chem.* **1992**, *67*, 337–348.
- (253) Sobczynski, A. *Monatsh. Chem.* **1991**, *122*, 645–652.
- (254) Foster, N. S.; Noble, R. D.; Koval, C. A. *Environ. Sci. Technol.* **1993**, *27*, 350–356.
- (255) Sayama, K.; Arakawa, H. *J. Phys. Chem.* **1993**, *97*, 531–533.
- (256) Aguado, M. A.; Gimenez, J.; Simarro, R.; Cerveramarch, S. *Solar Energy* **1992**, *49*, 47–52.
- (257) Frank, S. N.; Bard, A. J. *J. Am. Chem. Soc.* **1977**, *99*, 303–304.
- (258) Pollema, C. H.; Hendrix, J. L.; Milosavljevic, E. B.; Solujic, L.; Nelson, J. H. *J. Photochem. Photobiol. A: Chem.* **1992**, *66*, 235–244.
- (259) Rader, W. S.; Solujic, L.; Milosavljevic, E. B.; Hendrix, J. L.; Nelson, J. H. *Environ. Sci. Technol.* **1993**, *27*, 1875–1879.
- (260) Bhakta, D.; Shukla, S. S.; Chandrasekharaiah, M. S.; Margrave, J. L. *Environ. Sci. Technol.* **1992**, *26*, 625–626.
- (261) Frank, S. N.; Bard, A. J. *J. Phys. Chem.* **1977**, *81*, 1484–1488.
- (262) Maldotti, A.; Amadelli, R.; Bartocci, C.; Carassiti, V. *J. Photochem. Photobiol. A: Chem.* **1990**, *53*, 263–271.
- (263) Bamwenda, G. R.; Tsubota, S.; Kobayashi, T.; Haruta, M. *J. Photochem. Photobiol. A: Chem.* **1994**, *77*, 59–67.
- (264) Gao, Y. M.; Lee, W.; Trehan, R.; Kershaw, R.; Dwight, K.; Wold, A. *Mater. Res. Bull.* **1991**, *26*, 1247–1254.
- (265) Borgarello, E.; Harris, R.; Serpone, N. *Nouv. J. Chim.* **1985**, *9*, 743–746.
- (266) Serpone, N.; Borgarello, N.; Barbeni, M.; Pelizzetti, E.; Pichat, P.; Hermann, J. M.; Fox, M. A. *J. Photochem.* **1987**, *36*, 373–388.
- (267) Fitzmaurice, D. J.; Frei, H. *Langmuir* **1991**, *6*, 1129–1137.
- (268) Herrmann, J. M.; Pichat, P. *J. Chem. Soc., Faraday Trans. 1* **1980**, *76*, 1138–1146.
- (269) Micic, O. I.; Zhang, Y.; Cromack, K. R.; Trifunac, A. D.; Thurnauer, M. C. *J. Phys. Chem.* **1993**, *97*, 7277.
- (270) Serpone, N.; Ah-You, Y. K.; Tran, T. P.; Harris, R.; Pelizzetti, E.; Hidaka, H. *Solar Energy* **1987**, *39*, 491–498.
- (271) Tennakone, K.; Thaminimulle, C. T. K.; Senadeera, S.; Kumarasinghe, A. R. *J. Photochem. Photobiol. A: Chem.* **1993**, *70*, 193–195.
- (272) Ohtani, B.; Kakimoto, M.; Miyadzu, H.; Nishimoto, S.; Kagiya, T. *J. Phys. Chem.* **1988**, *92*, 5773–5777.
- (273) Hori, Y.; Nakatsu, A.; Suzuki, S. *Chem. Lett.* **1985**, 1429–1432.
- (274) Hori, Y.; Fujimoto, K.; Suzuki, S. *Chem. Lett.* **1986**, *9*, 1845–1848.
- (275) Kudo, A.; Sakata, T. *Chem. Lett.* **1992**, *12*, 2381–2384.
- (276) Yoneyama, H.; Shiota, H.; Tamura, H. *Bull. Chem. Soc. Jpn.* **1981**, *54*, 1308–1313.
- (277) Consesa, J. C.; Soria, J.; Augugliaro, V.; Palmisano, L. *Stud. Surf. Sci. Catal.* **1988**, *48*, 307.
- (278) Gonzalez-Elipse, A. R.; Munuera, G.; Soria, J. *J. Chem. Soc., Faraday Trans. 1* **1979**, *75*, 748.
- (279) Ohtani, B.; Zhang, S. W.; Ogita, T.; Nishimoto, S.; Kagiya, T. *J. Photochem. Photobiol. A: Chem.* **1993**, *71*, 195–198.
- (280) Ohtani, B.; Zhang, S. W.; Nishimoto, S.; Kagiya, T. *J. Chem. Soc., Faraday Trans. 1* **1992**, *88*, 1049–1053.
- (281) Mansilla, H. D.; Villasenor, J.; Maturana, G.; Baeza, J.; Freer, J.; Duran, N. *J. Photochem. Photobiol. A: Chem.* **1994**, *78*, 267–273.
- (282) Herrmann, J. M.; Disdier, J.; Pichat, P.; Fernandez, A.; Gonzalez-Elipse, A.; Munuera, G.; Leclercq, C. *J. Catal.* **1991**, *132*, 490–497.
- (283) Baciocchi, E.; Rosato, G. C.; Rol, C.; Sebastiani, G. V. *Tetrahedron Lett.* **1992**, *33*, 5437–5440.
- (284) Sclafani, A.; Palmisano, L.; Davi, E. *J. Photochem. Photobiol. A: Chem.* **1991**, *56*, 113–123.
- (285) Bahnemann, D. W. In *Sulfur Centered Reaction Intermediates in Chemical Biology*; 1990; pp 103–120.
- (286) Matsumoto, Y.; Nagal, H.; Sato, E. I. *J. Phys. Chem.* **1982**, *86*, 4664–4668.
- (287) Draper, R. B.; Fox, M. A. *J. Phys. Chem.* **1990**, *94*, 4628–4634.
- (288) Borgarello, E.; Serpone, N.; Grätzel, M.; Pelizzetti, E. *Hydrogen Energy* **1985**, *10*, 737–741.
- (289) Reeves, P.; Ohlhausen, R.; Sloan, D.; Pamplin, K.; Scoggins, T.; Clark, C.; Hutchinson, B.; Green, D. *Solar Energy* **1992**, *48*, 413–420.
- (290) Stephens, R. E.; Ke, B.; Trivich, D. *J. Phys. Chem.* **1955**, *59*, 966.
- (291) Pappas, S. P.; Fischer, R. M. *J. Paint Technol.* **1974**, *46*, 65.
- (292) Harbour, J. R.; Hair, M. L. *J. Phys. Chem.* **1977**, *81*, 1791.
- (293) Cundall, R. B.; Rudham, R.; Salim, M. S. *J. Chem. Soc., Faraday Trans. 1* **1976**, *72*, 1642.
- (294) Kormann, C.; Bahnemann, D. W.; Hoffmann, M. R. *J. Photochem. Photobiol. A: Chem.* **1989**, *48*, 161–169.
- (295) Pelizzetti, E.; Minero, C. *Electrochim. Acta* **1993**, *38*, 47–55.
- (296) Cunningham, J.; Al-Sayyed, G. *J. Chem. Soc., Faraday Trans. 1990*, *86*, 3935.
- (297) Wolff, K.; Bockelmann, D.; Bahnemann, D. In *Symposium on Electronic and Ionic Properties of Silver Halides: Common Trends with Photocatalysis*; Proceedings of the IS&T 44th Annual Conference; Levit, B., Ed.; IS&T: Springfield, VA, 1991; pp 259–267.
- (298) Neta, P.; Simic, M.; Hayon, E. *J. Phys. Chem.* **1969**, *73*, 4207–4213.
- (299) Choi, W.; Hoffmann, M. R. *Environ. Sci. Technol.* **1994**, submitted for publication.
- (300) Hilgendorff, M.; Bahnemann, D. W. In *Environmental Aspects of Electrochemistry and Photoelectrochemistry*; Tomkiewicz, M.; Haynes, R.; Yoneyama, H.; Hori, Y., Eds.; The Electrochemical Society: Pennington, 1993; pp 112–121.
- (301) Abdullah, M.; Low, G. K. C.; Matthews, R. W. *J. Phys. Chem.* **1990**, *94*, 6820.
- (302) Pelizzetti, E.; Carlin, V.; Minero, C.; Grätzel, M. *New J. Chem. (Nouv. J. Chim.)* **1991**, *15*, 351–359.
- (303) Martin, S. T.; Lee, A. T.; Hoffmann, M. R. *Environ. Sci. Technol.* **1994**, submitted for publication.
- (304) Minero, C.; Aliberti, C.; Pelizzetti, E.; Terzian, R.; Serpone, N. *Langmuir* **1991**, *7*, 928–936.
- (305) Grätzel, C. K.; Jirousek, M.; Grätzel, M. *J. Mol. Catal.* **1990**, *60*, 375–387.
- (306) Al-Ekabi, H.; Serpone, N.; Pelizzetti, E.; Minero, C.; Fox, M. A.; Draper, R. B. *Langmuir* **1989**, *5*, 250–255.
- (307) Pelizzetti, E.; Minero, C.; Carlin, V.; Borgarello, E. *Chemosphere* **1992**, *25*, 343–351.
- (308) Serpone, N.; Terzian, R.; Hidaka, H.; Pelizzetti, E. *J. Phys. Chem.* **1994**, *98*, 2634–2640.
- (309) Matthews, R. W. *Water Res.* **1990**, *24*, 653–660.
- (310) Hsieh, Y. H.; Wang, K. H. *Xingda Gongcheng Xuebao* **1992**, *3*, 103–110.
- (311) Matthews, R. W. *J. Catal.* **1988**, *111*, 264–272.
- (312) Matthews, R. W. *J. Phys. Chem.* **1987**, *91*, 3328–3333.
- (313) Tseng, J. M.; Huang, C. P. *Water Sci. Technol.* **1991**, *23*, 377–387.
- (314) Al-Sayyed, G.; Doliveira, J. C.; Pichat, P. *J. Photochem. Photobiol. A: Chem.* **1991**, *58*, 99–114.
- (315) Barbeni, M.; Pramauro, E.; Pelizzetti, E.; Borgarello, E.; Grätzel, M.; Serpone, N. *Nouv. J. Chim.* **1984**, *8*, 547.
- (316) Durand, A. P. Y.; Brattan, D.; Brown, R. G. *Chemosphere* **1992**, *25*, 783.
- (317) Haque, I. U.; Rusling, J. F. *Chemosphere* **1993**, *26*, 1301–1309.
- (318) Richard, C.; Boule, P. *New J. Chem.* **1994**, *18*, 547–552.
- (319) Vinodgopal, K.; Hotchandani, S.; Kamat, P. V. *J. Phys. Chem.* **1993**, *97*, 9040–9044.
- (320) Manilal, V. B.; Haridas, A.; Alexander, R.; Surender, G. D. *Water Res.* **1992**, *26*, 1035–1038.
- (321) Suri, R. P. S.; Liu, J.; Hand, D. W.; Crittenden, J. C.; Perram, D. L.; Mullins, M. E. *Water Environ. Res.* **1993**, *65*, 665–673.
- (322) Barbeni, M.; Morello, M.; Pramauro, E.; Pelizzetti, E. *Chemosphere* **1987**, *16*, 1165–1179.
- (323) Barbeni, M.; Pramauro, E.; Pelizzetti, E. *Chemosphere* **1985**, *14*, 195–208.
- (324) Minero, C.; Pelizzetti, E.; Malato, S.; Blanco, J. *Chemosphere* **1993**, *26*, 2103–2119.
- (325) Sabin, F.; Turk, T.; Vogler, A. *J. Photochem. Photobiol. A: Chem.* **1992**, *63*, 99–106.
- (326) Matthews, R. W. *Aust. J. Chem.* **1987**, *40*, 667–675.

- (327) Matthews, R. W.; Ollis, D. F. *J. Catal.* **1986**, *97*, 565-569.
- (328) Lepore, G.; Langford, C. H. *Water Pollut. Res. J. Can.* **1989**, *24*, 537-551.
- (329) Johnston, A. J.; Hocking, P. *ACS Symp. Series* **1993**, *518*, 106-118.
- (330) Barbeni, M.; Pramauro, E.; Pelizzetti, E. *Chemosphere* **1986**, *15*, 1913.
- (331) Pelizzetti, E.; Borgarello, M.; Minero, C.; Pramauro, E.; Borgarello, E.; Serpone, N. *Chemosphere* **1988**, *17*, 499-510.
- (332) Zhang, P. C.; Scudato, R. J.; Pagano, J. J.; Roberts, R. N. *Chemosphere* **1993**, *26*, 1213-1223.
- (333) Borello, R.; Minero, C.; Pramauro, E.; Pelizzetti, E.; Serpone, N.; Hidaka, H. *Environ. Toxicol. Chem.* **1989**, *8*, 997-1002.
- (334) Hidaka, H.; Nohara, K.; Zhao, J. C.; Takashima, K.; Pelizzetti, E.; Serpone, N. *New J. Chem.* **1994**, *18*, 541-545.
- (335) Hong, A. P.; Bahnemann, D. W.; Hoffmann, M. R. *J. Phys. Chem.* **1987**, *91*, 2109-2116.
- (336) Kuchmii, S. Y.; Kulik, S. V.; Korzhak, A. V.; Belous, A. I.; Kryukov, A. *Teor. Eksp. Khim.* **1989**, *25*, 682-688.
- (337) Navio, J. A.; Rives-Arnau, V. *Langmuir* **1990**, *6*, 1525-1526.
- (338) Kuhler, R. J.; Santo, G. A.; Caudill, T. R.; Betterton, E. A.; Arnold, R. G. *Environ. Sci. Technol.* **1993**, *27*, 2104-2111.
- (339) D'Oliveira, J. C.; Jayatilake, W.; Tennakone, K.; Herrmann, J. M.; Pichat, P. *Stud. Surf. Sci. Catal.* **1993**, *75*, 2167-2171.
- (340) Herrmann, J. M.; Guillard, C.; Pichat, P. *Catal. Today* **1993**, *17*, 7-20.
- (341) Bellobono, I. R.; Bonardi, M.; Catellano, L.; Selli, E.; Righetto, L. *J. Photochem. Photobiol. A: Chem.* **1992**, *67*, 109-115.
- (342) Tanaka, K.; Capule, M. F. V.; Higanaga, T. *Chem. Phys. Lett.* **1991**, *187*, 73-76.
- (343) Kondo, M. M.; Jardim, W. F. *Water Res.* **1991**, *25*, 823-827.
- (344) Nogueira, R.; Jardim, W. F. *J. Chem. Educ.* **1993**, *70*, 861-862.
- (345) Ahmed, S.; Ollis, D. F. *Solar Energy* **1984**, *32*, 597-601.
- (346) Pruden, A. L.; Ollis, D. F. *Environ. Sci. Technol.* **1983**, *17*, 628-631.
- (347) Tanguay, J. F.; Suib, S. L.; Coughlin, R. W. *J. Catal.* **1989**, *117*, 335-347.
- (348) Halmann, M.; Hunt, A. J.; Spath, D. *Solar Energy Mater. Solar Cells* **1992**, *26*, 1-16.
- (349) Tanaka, K.; Hisanaga, T.; Harada, K. *New J. Chem.* **1989**, *13*, 5-7.
- (350) Tausch, M. W.; Mundt, C.; Kehlenbach, V. *Prax. Naturwissen. Chem.* **1991**, *40*, 28-31.
- (351) Notthakun, S.; Crittenden, J. C.; Hand, D. W.; Perram, D. L.; Mullins, M. E. *J. Environ. Eng. Div. (ASCE)* **1993**, *119*, 695-714.
- (352) Dibble, L. A.; Raupp, G. B. *Catal. Lett.* **1990**, *4*, 345-354.
- (353) Mehos, M. S.; Turchi, C. S. *Environ. Prog.* **1993**, *12*, 194-199.
- (354) Tanaka, K.; Hisanaga, T.; Harada, K. *J. Photochem. Photobiol. A: Chem.* **1989**, *48*, 155-159.
- (355) Dieckmann, M. S.; Gray, K. A.; Kamat, P. V. *Water Sci. Technol.* **1993**, *25*, 277-279.
- (356) Low, G. K. C.; McEvoy, S. R.; Matthews, R. W. *Environ. Sci. Technol.* **1991**, *25*, 460-467.
- (357) Augugliaro, V.; Palmisano, L.; Schiavello, M.; Sclafani, A.; Marchese, L.; Matra, G.; Miano, F. *Appl. Catal.* **1991**, *69*, 323-340.
- (358) Palmisano, L.; Augugliaro, V.; Schiavello, M.; Sclafani, A. *J. Mol. Catal.* **1989**, *56*, 284-295.
- (359) Pelizzetti, E.; Carlin, V.; Minero, C.; Pramauro, E.; Vincenti, M. *Sci. Total Environ.* **1992**, *123*, 161-169.
- (360) Muszkat, L.; Halmann, M.; Raucher, D.; Bir, L. *J. Photochem. Photobiol. A: Chem.* **1992**, *65*, 409-417.
- (361) Pelizzetti, E.; Carlin, V.; Maurino, V.; Minero, C.; Dolci, M.; Marchesini, A. *Soil Sci.* **1990**, *150*, 523-526.
- (362) Pelizzetti, E.; Minero, C.; Carlin, V.; Pramauro, E.; Zervinatti, O.; Maurino, V.; Tosato, M. L. *Environ. Sci. Technol.* **1990**, *1559*-1565.
- (363) Dieckmann, M. S.; Gray, K. A.; Zepp, R. G. *Chemosphere* **1994**, *28*, 1021-1034.
- (364) Hustert, K.; Zepp, R. G. *Chemosphere* **1992**, *24*, 335-342.
- (365) Minoura, H.; Inayoshi, N.; Sugiura, T.; Ueno, Y.; Matsui, M.; Shibata, K. *J. Electroanal. Chem.* **1992**, *332*, 279-287.
- (366) Shibata, K.; Mimura, T.; Matsui, M.; Sugiura, T.; Minoura, H. *J. Chem. Soc., Chem. Commun.* **1988**, 1318-1320.
- (367) Brown, G. T.; Darwent, J. R. *J. Phys. Chem.* **1984**, *88*, 4955-4959.
- (368) Brown, G. T.; Darwent, J. R. *J. Chem. Soc., Faraday Trans. 1* **1984**, *80*, 1631-1643.
- (369) Matthews, R. W. *Water Res.* **1991**, *25*, 1169-1176.
- (370) Matthews, R. W. *J. Chem. Soc., Faraday Trans. 1* **1989**, *85*, 1291-1302.
- (371) Liu, X. S.; Lu, K. K.; Thomas, J. K. *J. Chem. Soc., Faraday Trans. 1* **1993**, *89*, 1861-1865.
- (372) Muzyka, J. L.; Fox, M. A. *J. Photochem. Photobiol. A: Chem.* **1991**, *57*, 27-39.
- (373) Bahnemann, D. W.; Fischer, C.; Janata, E.; Henglein, A. *J. Chem. Soc., Faraday Trans. 1* **1987**, *91*, 3782-3788.
- (374) Pramauro, E.; Vincenti, M.; Augugliaro, V.; Palmisano, L. *Environ. Sci. Technol.* **1993**, *27*, 1790-1795.
- (375) Fox, M. A.; Ogawa, H. *J. Inf. Rec. Mater.* **1989**, *17*, 351-361.
- (376) Low, G. K. C.; McEvoy, S. R.; Matthews, R. W. *Chemosphere* **1989**, *19*, 1611-1621.
- (377) Ohtani, B.; Nagasaki, H.; Sakano, K.; Nishimoto, S.; Kagiya, T. *J. Photochem. Photobiol. A: Chem.* **1987**, *41*, 141-143.
- (378) Anpo, M.; Aikawa, N.; Kubokawa, Y. *J. Phys. Chem.* **1984**, *88*, 3998-4000.
- (379) Nguyen, T.; Ollis, D. F. *J. Phys. Chem.* **1984**, *16*, 3386-3388.
- (380) Brezova, V.; Vodny, S.; Vesely, M.; Ceppan, M.; Lapcik, L. *J. Photochem. Photobiol. A: Chem.* **1991**, *56*, 125-134.
- (381) Horng, D. N.; Hsieh, H. K.; Liang, J. J. *Hua Hseuh* **1990**, *48*, 15-20.
- (382) Fujihira, M.; Staoh, Y.; Osa, T. *Nature* **1981**, *293*, 206-208.
- (383) Kato, T.; Maekawa, E.; Fujishima, A. *Stud. Org. Chem.* **1987**, *30*, 389-392.
- (384) Brezova, V.; Ceppan, M.; Brandsteterova, E.; Breza, M.; Lapeik, L. *J. Photochem. Photobiol. A: Chem.* **1991**, *59*, 385-391.
- (385) Izumi, I.; Fan, F. F.; Bard, A. J. *J. Phys. Chem.* **1981**, *85*, 218-223.
- (386) Terzian, R.; Serpone, N.; Minero, C.; Pelizzetti, E.; Hidaka, H. *J. Photochem. Photobiol. A: Chem.* **1990**, *55*, 243-249.
- (387) Brezova, V.; Brandsteterova, E.; Ceppan, M.; Pies, J. *Collect. Czech. Chem. Commun.* **1993**, *58*, 1285-1293.
- (388) Herrmann, J. M.; Mu, W.; Pichat, P. *Heterog. Catal. Fine Chem.* **1991**, *2*, 405-412; *Stud. Surf. Sci. Catal.* **1991**, *59*.
- (389) Halman, M. *J. Photochem. Photobiol. A: Chem.* **1992**, *66*, 215-223.
- (390) Ohtani, B.; Ueda, Y.; Nishimoto, S.; Kagiya, T.; Hachisuka, H. *J. Chem. Soc., Perkin Trans. 2* **1990**, 1955-1990.
- (391) Warman, J. M.; de Haas, M. P.; Pichat, P.; Serpone, N. *J. Phys. Chem.* **1991**, *95*, 8858.
- (392) Ait Ichou, I.; Formenti, M.; Pommier, B.; Teichner, S. J. *J. Catal.* **1985**, *91*, 293-307.
- (393) Cundall, R. B.; Hulme, B.; Rudham, R.; Salim, M. S. *J. Oil Colour Chem. Assoc.* **1978**, *61*, 351-355.
- (394) Henglein, A. *Ber. Bunsen-Ges. Phys. Chem.* **1982**, *86*, 241-246.
- (395) Green, K. J.; Rudham, R. *J. Chem. Soc., Faraday Trans.* **1992**, *88*, 3599-3603.
- (396) Ohtani, B.; Kakimoto, M.; Nishimoto, S.; Kagiya, T. *J. Photochem. Photobiol. A: Chem.* **1993**, *70*, 265-272.
- (397) Carlson, T.; Griffin, G. L. *J. Phys. Chem.* **1986**, *90*, 5896-5900.
- (398) Enea, O.; Ali, A. *New J. Chem.* **1988**, *12*, 853-858.
- (399) Liu, Y. C.; Griffin, G. L.; Chan, S. S.; Wachs, I. E. *J. Catal.* **1985**, *94*, 108-119.
- (400) Lepore, G. P.; Langford, C. H.; Vichova, J.; Vlcek, A. *J. Photochem. Photobiol. A: Chem.* **1993**, *75*, 67-75.
- (401) Matthews, R. W.; McEvoy, S. R. *Solar Energy* **1992**, *49*, 507-513.
- (402) Palmisano, L.; Schiavello, M.; Sclafani, A.; Matra, G.; Borello, E.; Coluccia, S. *Appl. Catal. B: Environ.* **1994**, *3*, 117-132.
- (403) Serpone, N.; Terzian, R.; Colarusso, P.; Minero, C.; Pelizzetti, E.; Hidaka, H. *Res. Chem. Intermed.* **1992**, *18*, 183-202.
- (404) Soria, J.; López-Munoz, M. J.; Augugliaro, V.; Conesa, J. C. *Colloid Surf. A: Phys. Eng.* **1993**, *78*, 73.
- (405) Trillas, M.; Pujol, M.; Domenech, X. *J. Chem. Technol. Biotechnol.* **1992**, *55*, 85-90.
- (406) Wei, T. Y.; Wang, Y. Y.; Wan, C. C. *J. Photochem. Photobiol. A: Chem.* **1990**, *55*, 115-126.
- (407) Wei, T. Y.; Wan, C. C. *J. Photochem. Photobiol. A: Chem.* **1992**, *69*, 241-249.
- (408) Augugliaro, V.; Davi, E.; Palmisano, L.; Schiavello, M.; Sclafani, A. *Appl. Catal.* **1990**, *65*, 101-116.
- (409) Sclafani, A.; Palmisano, L.; Schiavello, M. *J. Phys. Chem.* **1990**, *94*, 829-832.
- (410) Sclafani, A.; Palmisano, L.; Davi, E. *New J. Chem.* **1990**, *14*, 265-268.
- (411) King, J.; Zhi, P.; Chang, Q. *Synth. Met.* **1991**, *41*, 1139-1142.
- (412) Das, S.; Muneer, M.; Gopidas, K. R. *J. Photochem. Photobiol. A: Chem.* **1994**, *77*, 83-88.
- (413) Anpo, M.; Chiba, K.; Tomonari, M.; Coluccia, S.; Che, M.; Fox, M. A. *Bull. Chem. Soc. Jpn.* **1991**, *64*, 543-551.
- (414) Pichat, P.; Herrmann, J. M.; Disdier, J.; Mozzanega, M. N. *J. Phys. Chem.* **1979**, *83*, 3122-3126.
- (415) Walker, A.; Formenti, M.; Meriaudeau, P.; Teichner, S. J. *J. Catal.* **1977**, *50*, 237-243.
- (416) Navio, J. A.; Garcia-Gomez, M.; Pradera-Adrian, M.; Fuentes-Mota, J. *Stud. Surf. Sci. Catal.* **1991**, *59*, 445-453.
- (417) Vinodgopal, K.; Kamat, P. V. *J. Phys. Chem.* **1992**, *96*, 5053-5059.
- (418) Pelizzetti, E.; Minero, C.; Maurino, V.; Hidaka, H.; Serpone, N.; Terzian, R. *Ann. Chim.* **1990**, *80*, 81-87.
- (419) Pichat, P. *New J. Chem.* **1987**, *11*, 135-140.
- (420) Fox, M. A.; Abdel-Wahab, A. A. *J. Catal.* **1990**, *126*, 693-696.
- (421) Kraeutler, B.; Bard, A. J. *J. Am. Chem. Soc.* **1978**, *100*, 2239.
- (422) Sakata, T.; Kawai, T.; Hashimoto, K. *J. Phys. Chem.* **1984**, *88*, 2344-2350.
- (423) Kraeutler, B.; Bard, A. J. *J. Am. Chem. Soc.* **1978**, *100*, 5985-5992.

- (424) Kaise, M.; Kondo, H.; Nishihara, C.; Nozoye, H.; Shindo, H.; Nimura, S.; Kikuchi, O. *J. Chem. Soc., Chem. Commun.* **1993**, 395–396.
- (425) Sato, A. *J. Phys. Chem.* **1983**, *87*, 3531–3537.
- (426) Sato, A. *J. Chem. Soc., Chem. Commun.* **1982**, 26–27.
- (427) Pelizzetti, E.; Minero, C.; Maurino, V.; Sclafani, A.; Hidaka, H.; Serpone, N. *Environ. Sci. Technol.* **1989**, *23*, 1380–1385.
- (428) Pichat, P.; Herrmann, J. M.; Disdier, J.; Courbon, H.; Mozzanega, M. N. *Nouv. J. Chem.* **1981**, *5*, 629.
- (429) Goldberg, M. C.; Cunningham, K. M.; Weiner, E. R. *J. Photochem. Photobiol. A: Chem.* **1993**, *73*, 105–120.
- (430) Amadelli, R.; Bregola, M.; Polo, E.; Carassiti, V.; Maldotti, A. *J. Chem. Soc., Chem. Commun.* **1992**, 1355–1357.
- (431) Muzyka, J. L.; Fox, M. A. *J. Org. Chem.* **1990**, *55*, 209–215.
- (432) Fox, M. A.; Abdel-Wahab, A. A. *Tetrahedron Lett.* **1990**, *31*, 4533–4536.
- (433) Hidaka, H.; Yamada, S.; Suenaga, S.; Zhao, J.; Serpone, N.; Pelizzetti, E. *J. Mol. Catal.* **1990**, *59*, 279–290.
- (434) Zhao, J.; Oota, H.; Hidaka, H.; Pelizzetti, E.; Serpone, N. *J. Photochem. Photobiol. A.* **1992**, *69*, 251–256.
- (435) Daroux, M.; Klvana, D.; Duran, M.; Bideau, M. *Can. J. Chem. Eng.* **1985**, *63*, 668–673.
- (436) Formenti, M.; Juillet, F.; Meriaudeau, P.; Teichner, S. *J. Chem. Technol.* **1971**, 680–686.
- (437) Kato, K. *Bull. Chem. Soc. Jpn.* **1992**, *65*, 34–38.
- (438) Patel, K.; Yamagata, S.; Fujishima, A.; Loo, B. H.; Kato, T. *Ber. Bunsen-Ges. Phys. Chem. (Int. J. Phys. Chem.)* **1991**, *95*, 176–180.
- (439) Harada, H. *Chem. Exp.* **1991**, *6*, 961–964.
- (440) Tanaka, K.; White, J. M. *J. Phys. Chem.* **1982**, *86*, 4708–4714.
- (441) Matthews, R. W.; McEvoy, S. R. *J. Photochem. Photobiol. A.* **1992**, *66*, 355–366.

CR940170S